AD_____

Award Number: DAMD17-99-1-9205

TITLE: A Gene Amplification Phenotype in c-Myc-Induced Mammary Tumor Cells

PRINCIPAL INVESTIGATOR: Joon-Ho Sheen

CONTRACTING ORGANIZATION: Georgetown University Medical Center
Washington, DC 20057

REPORT DATE: July 2001

TYPE OF REPORT: Annual Summary

PREPARED FOR: U.S. Army Medical Research and Materiel Command
Fort Detrick, Maryland 21702-5012

REPORT DOCUMENTATION PAGE

Form Approved
OMB No. 074-0188

1. AGENCY USE ONLY (Leave blank)	2. REPORT DATE	3. REPORT TYPE AND DATES COVERED
	July 2001	Annual Summary (1 Jul 00 - 30 Jun 01)

4. TITLE AND SUBTITLE
A Gene Amplification Phenotype in c-Myc-Induced Mammary Tumor Cells

5. FUNDING NUMBERS
DAMD17-99-1-9205

6. AUTHOR(S)
Joon-Ho Sheen

7. PERFORMING ORGANIZATION NAME(S) AND ADDRESS(ES)

Georgetown University Medical Center
Washington, DC 20057

E-Mail: sheenj@goergetown.edu

8. PERFORMING ORGANIZATION REPORT NUMBER

9. SPONSORING / MONITORING AGENCY NAME(S) AND ADDRESS(ES)

U.S. Army Medical Research and Materiel Command
Fort Detrick, Maryland 21702-5012

10. SPONSORING / MONITORING AGENCY REPORT NUMBER

11. SUPPLEMENTARY NOTES
Report contains color

12a. DISTRIBUTION / AVAILABILITY STATEMENT
Approved for Public Release; Distribution Unlimited

12b. DISTRIBUTION CODE

13. ABSTRACT *(Maximum 200 Words)*
c-Myc has been implicated in breast cancer, as the oncoprotein is overproduced in nearly 80% of the disease. c-Myc constitutes a transcription factor, modulating transcription of cell-cycle-related genes and facilitating cell-cycle progression. Deregulated c-Myc also promotes genomic instability, that has been proposed as a driving force for tumorigenesis. For the creation of permissive conditions for gene amplification, a form of genomic instability, abrogation of cell-cycle checkpoints is recognized as a prerequisite. Checkpoint controls arrest cells containing DNA damage, such as broken chromosomes, which are important intermediates in gene amplification. The focus of the current study is the investigation of the c-Myc-induce alteration of DNA damage-induced checkpoints, creating permissive condition for the gene amplification phenotype. We carried out our studies with a set of mortal and immortal human mammary epithelial cell systems, established by retroviral transfection of empty vector, c-Myc, c-MycS, and p53DD. Using these cells, we demonstrated that the full-length c-Myc alters the DNA damage-induced checkpoints. This observation should help us to find novel targets for the prevention of gene amplification and for the arrest of proliferation of tumor cells with the deregulated c-Myc phenotype. The current research provided the PI with invaluable experience both conceptually and technically.

14. SUBJECT TERMS
Breast Cancer
c-Myc, Human Mammary Epithelial Cell, DNA damage-induced cell cycle checkpoints

15. NUMBER OF PAGES
88

16. PRICE CODE

17. SECURITY CLASSIFICATION OF REPORT	18. SECURITY CLASSIFICATION OF THIS PAGE	19. SECURITY CLASSIFICATION OF ABSTRACT	20. LIMITATION OF ABSTRACT
Unclassified	Unclassified	Unclassified	Unlimited

FOREWORD

Opinions, interpretations, conclusions and recommendations are those of the author and are not necessarily endorsed by the U.S. Army.

JH) Where copyrighted material is quoted, permission has been obtained to use such material.

JH) Where material from documents designated for limited distribution is quoted, permission has been obtained to use the material.

JH) Citations of commercial organizations and trade names in this report do not constitute an official Department of Army endorsement or approval of the products or services of these organizations.

N/A In conducting research using animals, the investigator(s) adhered to the "Guide for the Care and Use of Laboratory Animals," prepared by the Committee on Care and use of Laboratory Animals of the Institute of Laboratory Resources, national Research Council (NIH Publication No. 86-23, Revised 1985).

JB For the protection of human subjects, the investigator(s) adhered to policies of applicable Federal Law 45 CFR 46.

NA In conducting research utilizing recombinant DNA technology, the investigator(s) adhered to current guidelines promulgated by the National Institutes of Health.

NA In the conduct of research utilizing recombinant DNA, the investigator(s) adhered to the NIH Guidelines for Research Involving Recombinant DNA Molecules.

NA In the conduct of research involving hazardous organisms, the investigator(s) adhered to the CDC-NIH Guide for Biosafety in Microbiological and Biomedical Laboratories.

J. Sloan 9/30/01

PI - Signature Date

Table of Contents

For Annual Report Grant #DAMD17-99-1-9205
"A Gene Amplification Phenotype in c-Myc-induced Mammary Tumor Cells"

This Annual Summary Report addresses Grant # DAMD17-99-1-9205, a Pre-Doctoral Training Fellowship, covering research conducted by the principal investigator Joon-Ho Sheen (a Ph.D. student at the Lombardi Cancer Center, Georgetown University Medical Center), entitled "A Gene Amplification Phenotype in c-Myc-Induced Mammary Tumor Cells."

INTRODUCTION:

The *c-myc* oncogene is particularly implicated for breast cancer. This oncogene *per se* is amplified in the approximately 30% of the human breast tumor cases, while the c-Myc oncoprotein is overproduced or deregulated in nearly 80% of the disease (Bonilla et al., 1988; Escot et al., 1986). This wide prevalence of c-Myc defects suggests the importance of this oncogene in the genesis and/or progression of breast cancer. The c-Myc oncoprotein consists of 439 amino acid residues. In terms of protein structure of c-Myc, the oncoprotein has highly conserved domains among the species, so called MB-I (Myc-Box I) and MB-II (Myc-Box II), in its N-terminal transactivation region. Furthermore, previous studies showed that both MB-I and MB-II are required for the c-Myc-induced transactivation. However, only MB-II is required for the c-Myc-induced repression. Interestingly, a naturally truncated form of c-Myc, named c-MycS, has only MB-II in the transactivation region since its translation starts at the internal AUG initiation codon, located between MB-I and MB-II domain (Spotts et al., 1997; Xiao et al., 1998). Functionally, c-Myc forms a nuclear transcription factor that interacts with DNA, when heterodimerized with the partner protein MAX. This heterodimerization, through the interaction of C-terminal leucine zipper and basic helix-loop-helix motifs, is required for c-Myc-mediated cell cycle progression, cell growth, cellular transformation, and apoptosis (Dang et al., 1989). However, in addition to the already established roles of c-Myc, recent studies have suggested a novel role of the oncoprotein, a c-Myc-induced genomic instability phenotype. The development of the malignant breast cancer phenotype may depend upon the stepwise accumulation of genetic changes, as is the case in other types of tumors (Nowell, 1976; Vogelstein and Kinzler, 1993). Genomic instability in tumor cells has been proposed and investigated as a driving force for the step-wise development of the cancer phenotype by facilitating the accumulation of necessary genetic changes (Loeb, 1991; Tlsty et al., 1995). Therefore, understanding the mechanisms for genomic instability phenotype would provide important insights into the progression of breast cancer and into potential ways to prevent it. Specifically, genomic instability phenotype at the level of gene amplification has been implicated in the development of drug resistance and metastatic potential (Lucke-Huhle, 1994). Since the major causes of morbidity of breast tumors are metastasis and drug resistance, it is crucial to know how normal mammary epithelial cells acquire the gene amplification phenotype for the prevention and the treatment of these malignant phenotypes. Gene amplification is a complex mechanical process, including chromosomal breakage, losses of chromosome region, and gains of chromosome region (Stark, 1993). A widely accepted explanation for the gene amplification phenotype is based on the altered cell cycle, resulting from the abrogation of a cell cycle checkpoint(s)(Hartwell et al., 1994; Paulovich et al., 1997). Checkpoint control is a feedback signal for the ordered cell cycle progression, insuring the completion of one process prior to initiating a downstream process (Hartwell, 1992; Hartwell et al., 1994; Paulovich et al., 1997). Mutations of the feedback-signaling

pathway will therefore predispose for the disarray of the cell cycle. Among the various checkpoints, the DNA-damage checkpoint(s) has been implicated crucially in the prevention of gene amplification (Ishizaka et al., 1995; Wahl et al., 1997; Wright et al., 1990). The inappropriate entry of damaged DNA into S-phase, in the absence of checkpoint control, will eventually amplify DNA damage during the unprepared DNA replication (Almasan et al., 1995). Failure of the cell to detect damaged DNA and the subsequent arrest of cells at the checkpoint could create permissive conditions for the accumulation of further DNA damage, such as double-strand DNA breakage. Furthermore, broken chromosomes resulting from the double-strand DNA breakage, possibly induced by ionizing radiation and/or DNA-damaging chemotherapeutic drugs, have been by far the most effective inducers for the gene amplification process (Smith et al., 1992; Smith et al., 1995; Windle et al., 1991). However, in normal cells with intact checkpoint controls, broken chromosomes are monitored and eliminated so that the gene amplification could not occur. Cells with DNA damage are arrested and destined to undergo apoptosis. The DNA damage-induced checkpoint detects even a single double-strand break and permanently arrests cells containing DNA damage. Therefore, abrogation of checkpoint controls is a prerequisite for a gene amplification phenotype (Di Leonardo et al., 1993). Interestingly, my preliminary study with the c-Myc-induced mouse mammary carcinoma cells indicates an increased frequency of *CAD* gene amplification as well as alterations of several checkpoint controls. I thus proposed that deregulated c-Myc creates permissive conditions for the gene amplification phenotype through bypassing cell cycle checkpoints. As an experimental approach, I employed both the full-length c-*myc* and the transrepression-only c-*mycS* constructs to dissect the effects of c-Myc on the DNA damage-induced checkpoints. c-MycS has provided a chance to determine whether the 'transactivation' of c-Myc targets is essential for the c-Myc-induced effects on the cell cycle checkpoint control. Furthermore, p53DD, a dominant negative form of tumor suppressor p53, has been employed to serve as a positive control for the abrogated checkpoint phenotype in human mammary epithelial cells (HMEC). The central involvement of p53 is well established in the DNA damage-induced checkpoints. Genomic instability phenotype has been implicated in tumor initiation as well as in the malignant progression to more advanced malignancies. Therefore, results from this study would provide useful information about the development of mammary tumors induced by deregulated c-Myc. Essentially, this pre-doctoral research project has provided me with an invaluable opportunity to think seriously about how a specific oncogene promotes tumor progression in the mammary tissues at the molecular level. The proposed study also has allowed me to learn cellular and molecular genetic research tools, such as the recombinant DNA technology, retroviral transfection for cell line establishment, and flow cytometry. These conceptual and technical advances have led me to a Ph.D. degree and provided me an invaluable background experience for my future as an independent scientist focusing on breast cancer research.

BODY OF SUMMARY REPORT:

This is the second Annual Summary Report (and proposed Final Report) of Training and Research Accomplishments for this grant (the period between July 1, 2000 and June 30, 2001) of a 3 year pre-doctoral training grant # DAMD17-99-1-9205 for Joon-Ho Sheen. Please note that a revised statement of work will be presented within this summary discussion, describing the completion of the Specific Aims within a period of time shorter than initially anticipated. Accordingly, Joon-Ho Sheen recently received his Ph.D. degree, based on training and research accomplishments through this pre-doctoral traineeship.

The first annual report, covering the first year (the period between July 1, 1999 and June 30, 2000), described the research, performed according to the revised and approved specific aim #1. For this second report, a revision of specific aims #2 and #3 are now requested to emphasize more the study of effects of c-Myc expression on the cell cycle checkpoints (original specific aims #1D and #3B). In addition, these revised aims are consistent with the directives of the faculty members on my Ph.D. Thesis Committee. The revision reflects a consistent and continuous effort to establish the direct causality between c-Myc and the DNA damage-induced cell cycle checkpoint alteration, which were described in the previously revised specific aim #1 in the first annual report. The establishment of regulatable Myc (c-MycER^{TM}) system in the background of HMEC line (original specific aim #2A) and the use of mortal HMEC system (newly added to specific aim #2) are representative major accomplishments in this research period. These systems have allowed us to draw a strong conclusion on the effects of c-Myc expression on the cell cycle checkpoints, providing a firm base for the next analysis for the c-Myc-induced genomic instability phenotype. We believe that the study of the c-Myc-induced alteration(s) of the DNA damage-induced checkpoint(s) at G1/S and G2/M boundary is very important, and further studies are urgently needed to elucidate the 'prerequisites' and the 'fundamental mechanism(s)' for genomic instability phenotype at the level of gene amplification.

I. The first annual summary report (period between July 1, 1999 and June 30, 2000)

Revised (and Approved) Specific Aim #1: To characterize a c-Myc-induced checkpoint alteration at G1/S in Human Mammary Epithelial Cells (HMEC) *(Months 1-18)*. **[Completed in Year 1]**

A. To establish an experimental system consisting of a set of HMECs transfected with c-Myc and c-MycS.
B. To characterize the cell cycle checkpoint controls at G1/S boundary responding to γ-irradiation-induced DNA damage in the above HMEC system through the flow cytometric analysis.

II. The second annual summary report (period between July 1, 2000 and June 30, 2001)

Original Specific Aim #2: To determine if a direct causal relationship exists between c-Myc expression and the gene amplification phenotype. *(Months 12-30)*. **[Now Requested Revision, below]**

A. To express a regulatable c-Myc construct in mammary epithelial cells.
B. To determine whether the conditional overexpression of c-Myc activity increases the frequency of drug resistant cells.
C. To determine whether the drug resistant subclones have the amplification of indicator genes.
D. To determine whether the DNA-damaging agents can significantly stimulate the accumulation of gene amplifications in cells conditionally overexpressing c-Myc.

Revised Specific Aim #2: To determine if a direct causality exists between c-Myc expression and the checkpoint alteration phenotype. *(Months 12-24)*. **[Now Completed in Year 2]**

A. To express a regulatable c-Myc construct in mammary epithelial cell line.
B. To determine whether the conditional excess of c-Myc activity alters the G1/S arrest following γ-irradiation-induced DNA damage.
C. To establish a normal mortal HMEC system transiently transfected with c-Myc, c-MycS, or p53DD construct.
D. To determine whether the transient expression of c-Myc alters the G1/S arrest following γ-irradiation-induced DNA damage in the background of normal mortal HMEC.

Original Specific Aim #3: To study the time-course of the c-Myc-induced gene amplification phenotype. *(Months 24-36)*. **[Now Requested Revision, below]**

A. To determine how fast the conditional overexpression of c-Myc increases gene amplifications in normal culture condition.
B. To determine how fast the conditional overexpression of c-Myc activity abrogates cell cycle checkpoint controls.

Revised Specific Aim #3: To characterize effects of c-Myc overexpression on the checkpoint at G2/M boundary. *(Months 12-24)*. **[Now Completed in Year 2]**

A. To characterize the DNA damage-induced micronuclei formation, selectively, in c-Myc-overexpressing HMECs.
B. To characterize effects of c-Myc overexpression on the G2/M transition and the cell division.

Training and Research Accomplishments for Specific Aims #2 and #3 (as Revised):

In this second year of training and research (the period between July 1, 2000 and June 30, 2001), we were able to establish the causality between c-Myc and altered checkpoint by employing the MCF10A expressing regulatable MycER^{TM} (Revised specific aim #2A and #2B). The c-Myc-induced checkpoint alteration was also observed in finite lifespan, normal HMECs after transient expression of c-Myc from a retroviral construct (Revised specific aim #2C and #2D). Results from these studies were submitted for publication (Sheen and Dickson, 2001a). For the experimental details, please see the attached manuscript in Appendix.

Two representative DNA damage-induced checkpoints are at G1/S (preventing inappropriate replication of damaged DNA) and at G2/M (preventing segregation of damaged chromosomes). Therefore, we determined to investigate effects of c-Myc overexpression on the G2/M arrest and mitotic division following DNA damage (Sheen and Dickson, 2001a).(Sheen and Dickson, 2001b) MCF10A-MycER^{TM} cells (MCF10A cells, infected with a regulatable c-MycER^{TM} construct) were irradiated in the presence of EtOH (a vehicle control) or 4-OHT (4-hydroxy-tamoxifen). The activity of c-MycER^{TM} could be selectively activated by addition of an estrogen receptor-binding ligand, 4-OHT (Sheen and Dickson, 2001a). After prolonged (48 to 72 hrs) post-IR incubation, following 12 Gray IR, cellular morphologies were examined by phase-contrast microscopy. Interestingly, a significant fraction of the 4-OHT-treated cells (roughly 40 % of total) contained micronuclei **(black arrows in Figure 1)**. The formation of micronuclei has been reported to be a 'post-mitotic' event, eventually undergoing apoptosis in some cells (Forrester et al., 1999; Forrester et al., 2000; Vidair et al., 1996). Therefore, the dramatic induction of micronuclei after IR, selectively in cells with activated c-MycER^{TM}, suggest the possibility of c-Myc-induced alteration of G2/M arrest following DNA damage. To characterize further the post-IR induction of micronuclei, following 12 Gray IR, cells were plated in culture media containing an artificial nucleotide analog, BrdU, in the presence or absence of 4-OHT. After 48 hrs of post-IR incubation, incorporation of BrdU was examined under fluorescence microscopy. As expected, BrdU incorporation was identified selectively in cells treated with 4-OHT, following γ-irradiation, as activated c-Myc alter the G1/S checkpoint. Furthermore, some of the micronuclei **(yellow arrows in Figure 2)** and mitotic chromosomes **(white arrows in Figure 2)** contained BrdU-positive, *de novo* synthesized DNA. Thus, following IR, some damaged DNA had undergone replication and managed to reach to the stage of micronucleation. Taken together, these results also supported the possibility that c-Myc may alter both G1/S and G2/M-entry checkpoints. To determine whether c-Myc overexpression alters the DNA damage-induced checkpoint at G2/M, we performed a mitotic trapping assay (Bunz et al., 1998) with MCF10A infected with the empty LXSN retroviral vector, or the LXSN vector containing c-*myc*, c-*mycS*, or *p53DD*. Following 0 Gray or 4 Gray of γ-irradiation to the culture dishes, media were replaced with complete media, supplemented with nocodazole, a microtubule (MT)-destabilizing drug. The treatment of cells with nocodazole immediately establishes a chemical trap in the middle of mitosis because cells arrest temporarily at M phase. In the absence of mitotic spindles (nocodazole treatment), the transition from metaphase to anaphase is blocked, and cells are trapped temporarily in the middle of M-phase. Therefore, the number of cells that entered into M phase over a certain time-period can be easily amplified for the convenience of measurement **(Figure 3)**. The rounded-up morphology is a shape typical of cells undergoing mitosis **(Figure 4)**. A clear identification of rounded-up mitotic morphology was evident. After 36 hr post- 0 Gray incubation plus nocodazole treatment, both MCF10A-LXSN (MCF10A cells infected with LXSN empty retroviral vector) and MCF10A-MycS (MCF10A infected with c-*MycS*) demonstrated that approximately 10% of total cells were rounded-up. However, following 4 Gray IR, a dramatic decrease (to less than 1%) of rounded-up cells were observed (roughly 90% reduction of rounded-up mitotic cells). This is consistent with an interpretation that both MCF10A-LXSN and MCF10A-MycS cells maintain a functional G2/M checkpoint. In contrast, MCF10A-Myc

(MCF10A cells infected with full-length c-*Myc*) and MCF10A-p53DD (MCF10A cells infected with *p53DD*, encoding a dominant negative p53 mini-protein) demonstrated a significant accumulation of rounded-up cells even after γ-irradiation. Following the 4 Gray IR, the percentages of rounded-up cells were clearly maintained in MCF10A-c-Myc (approximately 30% in non-irradiated and 10% in irradiated, 66% reduction of rounded-up cells by IR) and MCF10A-p53DD (approximately 20% in non-irradiated and 10% in irradiated, 50% reduction of rounded-up cells by IR). Therefore, although further analyses are required to quantitate and validate the alteration of G2/M checkpoint by c-Myc or p53DD, these results support the postulate that c-Myc overexpression or loss of p53 is each sufficient to attenuate the G2/M arrest, following IR-induced DNA damage. To address directly the alteration of the post-IR transition from G2 to M in c-Myc-overexpressing cells, time-lapse videomicroscopy was employed. Under, 0 Gray, no DNA damage controls, MCF10A-MycER^{TM} cells exhibited apparently normal mitoses, as well as balanced cytokineses. However, after post-IR incubation, some cells demonstrated aberrant mitoses of both a prolonged nature and with unbalanced cytokineses **(Figure 4)**.

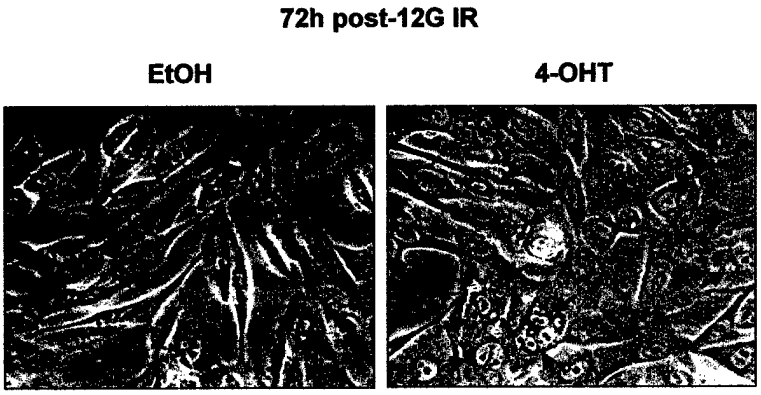

Figure 1. Micronucleation after prolonged post-IR incubation of 4-OHT-stimulated MCF10A-MycER^{TM} cells.

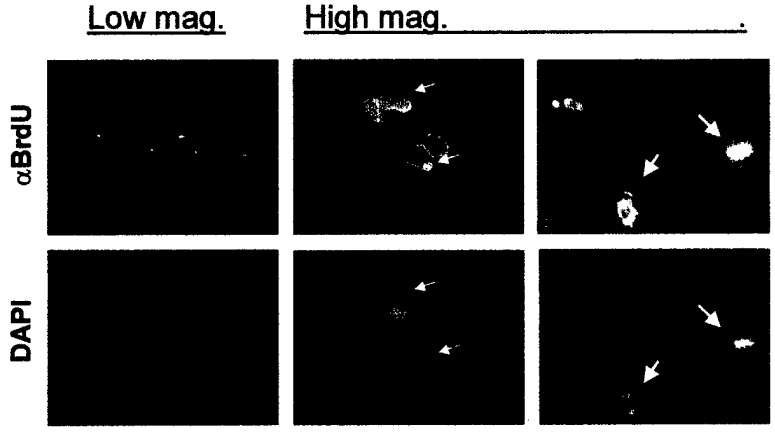

Figure 2. DNA damage-induced micronuclei contain *de novo* synthesized DNA.

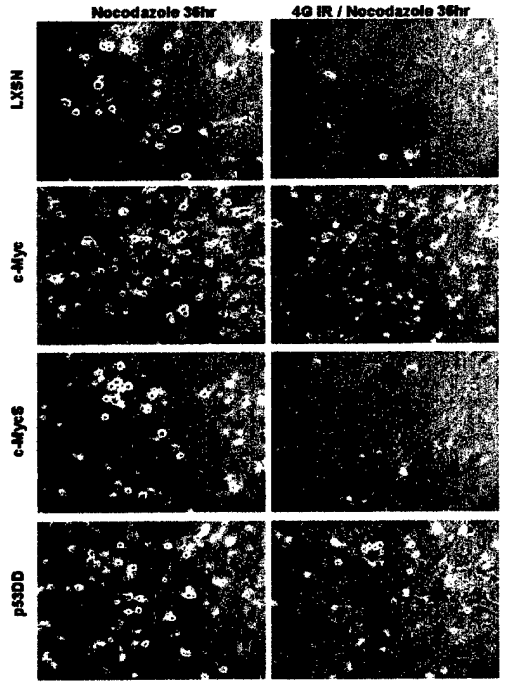

Figure 3. The mitotic trapping assay.

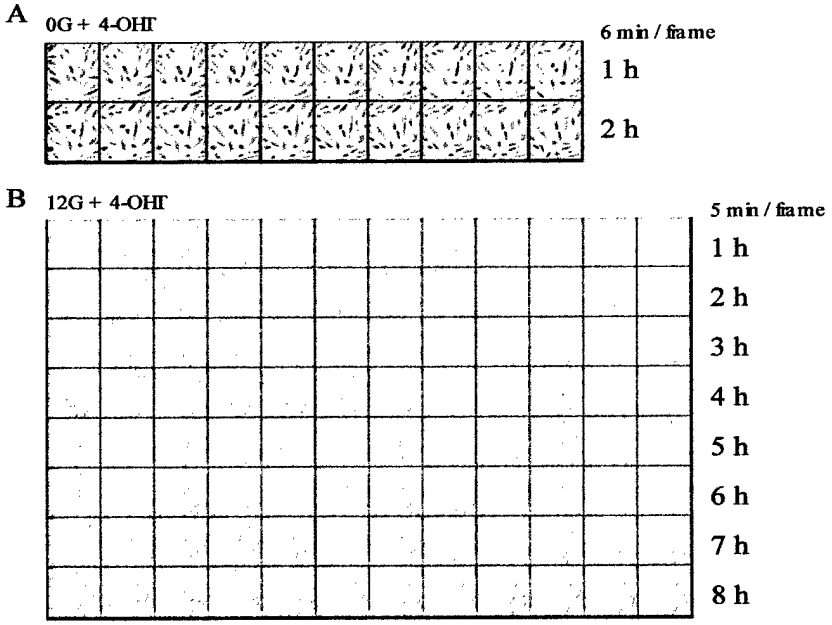

Figure 4. Aberrant mitotic divisions following ionizing radiation in 4-OHT-stimulated MCF10A-MycER^{TM} cells.

KEY RESEARCH ACCOMPLISHMENTS for GRANT # DAMD17-99-1-9205:

The 184A1N4 immortalized HMEC line study:

- Characterization of the DNA damage-induced checkpoint at G1/S in the 184A1N4, a chemically immortalized, HMEC line, with the employment of γ-irradiation.

- Identification of the abrogated G1/S checkpoint in the c-Myc-overexpressing, 184A1N4-Myc HMEC line.

The MCF10A immortalized HMEC line study:

- Characterization of the DNA damage-induced checkpoint at G1/S in the MCF10A, a spontaneously immortalized HMEC line, with the employment of γ-irradiation.

- Establishment of the MCF10A system, expressing full-length *c-myc*, *c-mycS*, or *p53DD* construct, *via* retroviral gene transfection techniques.

- Identification of the attenuated G1/S arrest following DNA damage in the c-Myc-overexpressing MCF10A HMEC line, which is consistent with the results from 184A1N4-Myc HMEC line.

- Identification of two specific regions of the c-Myc protein (MB-I and MB-II) that are required to attenuate the DNA damage-induced G1/S checkpoint in HMEC line.

- Characterization of altered G1/S checkpoint response by time-course western analysis; deregulated hyperphosphorylation of Rb and inappropriate upregulation of cyclin A were identified, following DNA damage, in c-Myc- or p53DD-overexpressing cells.

- Establishment of the regulatable Myc system in MCF10A HMEC line, by transfecting *c-mycER*^{TM} construct that could be activated by addition of 4-OHT.

- Identification of the attenuated G1/S arrest following DNA damage, selectively, in 4-OHT-stimulated MCF10A-MycER cells, indicating direct effects of c-Myc on the DNA damage-induced checkpoint at G1/S.

- Identification of the micronucleation and aberrant mitoses following DNA damage, selectively, in 4-OHT-stimulated MCF10A-MycER cells, suggesting a potential effect of deregulated c-Myc on the alteration of G2/M transition and mitosis following DNA damage.

Normal HMEC study:

- Establishment of the normal mortal HMEC system, expressing full-length *c-myc*, *c-mycS*, or *p53DD*, transiently, *via* retroviral gene transfection techniques.

- Identification of the attenuated G1/S arrest, following DNA damage, selectively, in the full-length c-myc or p53DD-expressing cells, indicating the consistent effects of full-length c-Myc on the DNA damage-induced checkpoint at G1/S, in normal HMECs.

- Identification of the micronucleation and aberrant mitoses following DNA damage, selectively, in the full-length c-myc or p53DD-expressing cells, suggesting a potential effect of deregulated c-Myc on the alteration of G2/M transition and mitosis following DNA damage, in normal HMECs.

REPORTABLE OUTCOMES LIST for GRANT # DAMD17-99-1-9205:

Presentation Abstracts:

1. Joon-Ho Sheen and Robert B. Dickson. Deregulated c-Myc alters DNA damage-dependent G1/S checkpoint. Georgetown University Medical Center and Lombardi Cancer Center Research Poster Day. February 2000.

- ❑ Copy of Abstract Attached in the Appendix.

2. Joon-Ho Sheen and Robert B. Dickson. Deregulated c-Myc induces alteration of DNA damage-dependent G1/S checkpoint in human mammary epithelial cells. Abstract #2793. 91st Annual Meeting of American Association for Cancer Research. April 2000, San Francisco, CA.

- ❑ Copy of Abstract Attached in the Appendix.

Manuscripts for publication:

1. Joon-Ho Sheen and Robert B. Dickson. 2001. Effects of c-Myc expression on G2/M arrest and aberrant mitosis following DNA damage. **In preparation.**

- ❑ Copy of Abstract Attached in the Appendix.

2. Joon-Ho Sheen and Robert B. Dickson. 2001. c-Myc alters the DNA damage-induced checkpoint at G1/S. **Submitted.**

- ❑ Copy of the Manuscript submitted Attached in the Appendix.

Degree obtained:

1. Joon-Ho Sheen. July 2001. Effects of c-Myc expression on the DNA damage-induced cell cycle checkpoints. **Ph.D. thesis dissertation, Department of Cell Biology, Georgetown University, Washington, DC.**

- ❑ Copy of Abstract Attached in the Appendix.

CONCLUSIONS:

During this second year of work on the pre-doctoral training grant # DAMD17-99-1-9205 by Joon-Ho Sheen, effects of c-Myc expression were investigated on the DNA damage-induced checkpoints at the G1/S and at the G2/M boundaries in human mammary epithelial cells (HMECs). A transient excess of c-Myc activity, *via* the regulatable c-MycER, was, similarly, able to attenuate G1/S arrest, following ionizing radiation (IR). The c-Myc-induced G1/S alteration was also observed in finite lifespan, normal HMECs. In a molecular analysis, we observed deregulated hyperphosphorylation of Rb and then the reappearance of cyclin A, as the c-Myc-overexpressing cells entered into S phase, following IR. One additional finding from G1/S study is a dramatic increase in the cellular contents of multiple micronuclei, following IR, selectively in cells with excess c-Myc activity. Since micronucleation is a post-mitotic event, the results suggest a possibility of altered G2/M checkpoint by c-Myc. Therefore, we hypothesized that c-Myc alters the G2/M checkpoint, as well. We investigated the effects of c-Myc overexpression on the G2/M arrest following IR by employing a mitotic trapping assay, and obtained pilot data supporting our hypothesis. The MCF10A cells, overexpressing either c-Myc or dominant negative p53DD, demonstrated a significant percentage of cells in mitosis, following prolonged post-IR incubation with nocodazole. In contrast, cells infected with an empty vector or a c-MycS-containing vector did not show significant numbers of rounded-up cells. Finally, mitoses of irradiated MCF10A-MycER cells were directly examined by time-lapse videomicroscopy. After prolonged mitoses, following IR, mitotic cells eventually were observed to carry out unbalanced cytokineses. Taken together, these results suggest that c-Myc alters safeguard mechanisms for genomic stability, both at the G1/S and at the G2/M boundaries. Alterations of the DNA damage-induced checkpoints, such as the one studied here, have been identified as crucial prerequisites for certain types of genomic instability, such as gene amplification. Therefore, based on these findings, we propose that deregulated c-Myc abrogates a safeguard mechanism(s) for genomic stability. The principal investigator, Joon-Ho Sheen, received his Ph.D. degree, successfully, based on the significant training and research accomplishments through this invaluable opportunity provided by the pre-doctoral traineeship of Army breast cancer research program.

REFERENCES:

Almasan,A., Linke,S.P., Paulson,T.G., Huang,L.C., and Wahl,G.M. (1995). Genetic instability as a consequence of inappropriate entry into and progression through S-phase. Cancer Metastasis Rev *14*, 59-73.

Bonilla,M., Ramirez,M., Lopex-Cueto,J., and Gariglio,P. (1988). In vivo amplification and rearrangement of c-myc oncogene on human breast tumors. J Natl Cancer Inst *80*, 665-671.

Bunz,F., Dutriaux,A., Lengauer,C., Waldman,T., Zhou,S., Brown,J.P., Sedivy,J.M., Kinzler,K.W., and Vogelstein,B. (1998). Requirement for p53 and p21 to sustain G2 arrest after DNA damage. Science *282*, 1497-1501.

Dang,C.V., McGuire,M., Buckmire,M., and Lee,W.M. (1989). Involvement of the 'leucine zipper' region in the oligomerization and transforming activity of human c-myc protein. Nature *337*, 664-6.

Di Leonardo,A., Linke,S.P., Yin,Y., and Wahl,G.M. (1993). Cell cycle regulation of gene amplification. Cold Spring Harb Symp Quant Biol *58*, 655-67.

Escot,C., Theillet,C., Liderau,R., Spyratos,F., Champeme,M., Gest,J., and Callahan,R. (1986). Genetic alteration of the c-myc protooncogene (MYC) in human primary breast carcinomas. Proc Natl Acad Sci USA *83*, 4834-4838.

Forrester,H.B., Albright,N., Ling,C.C., and Dewey,W.C. (2000). Computerized video time-lapse analysis of apoptosis of REC:Myc cells X-irradiated in different phases of the cell cycle. Radiat. Res. *154*, 625-639.

Forrester,H.B., Vidair,C.A., Albright,N., Ling,C.C., and Dewey,W.C. (1999). Using computerized video time lapse for quantifying cell death of X-irradiated rat embryo cells transfected with c-myc or c-Ha-ras. Cancer Res. *59*, 931-939.

Hartwell,L. (1992). Defects in a cell cycle checkpoint may be responsible for the genomic instability of cancer cells. Cell *71*, 543-6.

Hartwell,L., Weinert,T., Kadyk,L., and Garvik,B. (1994). Cell cycle checkpoints, genomic integrity, and cancer. Cold Spring Harb Symp Quant Biol *59*, 259-63.

Ishizaka,Y., Chernov,M.V., Burns,C.M., and Stark,G.R. (1995). p53-dependent growth arrest of Ref52 cells containing newly amplified Dna. Proc Natl Acad Sci U S A *92*, 3224-8.

Loeb,L.A. (1991). Mutator phenotype may be required for multistage carcinogenesis. Cancer Res *51*, 3075-9.

Lucke-Huhle,C. (1994). Permissivity for methotrexate-induced DHFR gene amplification correlates with the metastatic potential of rat adenocarcinoma cells. Carcinogenesis *15*, 695-700.

Nowell,P. (1976). The clonal evolution of tumor cell populations. Science *194*, 23-28.

Paulovich,A.G., Toczyski,D.P., and Hartwell,L.H. (1997). When checkpoints fail. Cell *88*, 315-321.

Sheen,J. and Dickson,R.B. (2001a). c-Myc alters the DNA damage-induced checkpoint at G1/S. Submitted.

Sheen,J. and Dickson,R.B. (2001b). Effects of c-Myc expression on G2/M arrest and aberrant mitosis following DNA damage. In preparation.

Smith,K.A., Agarwal,M.L., Chernov,M.V., Chernova,O.B., Deguchi,Y., Ishizaka,Y., Patterson,T.E., Poupon,M.F., and Stark,G.R. (1995). Regulation and mechanisms of gene amplification. Philos Trans R Soc Lond B Biol Sci *347*, 49-56.

Smith,K.A., Stark,M.B., Gorman,P.A., and Stark,G.R. (1992). Fusions near telomeres occur very early in the amplification of CAD genes in Syrian hamster cells. Proc Natl Acad Sci U S A *89*, 5427-31.

Spotts,G.D., Patel,S.V., Xiao,Q., and Hann,S.R. (1997). Identification of downstream-initiated c-Myc proteins which are dominant-negative inhibitors of transactivation by full-length c-Myc proteins. Mol. Cell Biol. *17*, 1459-1468.

Stark,G.R. (1993). Regulation and mechanisms of mammalian gene amplification. Adv Cancer Res *61*, 87-113.

Tlsty,T.D., Briot,A., Gualberto,A., Hall,I., Hess,S., Hixon,M., Kuppuswamy,D., Romanov,S., Sage,M., and White,A. (1995). Genomic instability and cancer. Mutat Res *337*, 1-7.

Vidair,C.A., Chen,C.H., Ling,C.C., and Dewey,W.C. (1996). Apoptosis induced by X-irradiation of rec-myc cells is postmitotic and not predicted by the time after irradiation or behavior of sister cells. Cancer Res. *56*, 4116-4118.

Vogelstein,B. and Kinzler,K.W. (1993). The multistep nature of cancer. Tren. In Gen. *9*, 138-141.

Wahl,G.M., Linke,S.P., Paulson,T.G., and Huang,L.C. (1997). Maintaining genetic stability through TP53 mediated checkpoint control. Cancer Surv *29*, 183-219.

Windle,B., Draper,B.W., Yin,Y.X., S,O.G., and Wahl,G.M. (1991). A central role for chromosome breakage in gene amplification, deletion formation, and amplicon integration. Genes Dev *5*, 160-74.

Wright,J.A., Smith,H.S., Watt,F.M., Hancock,M.C., Hudson,D.L., and Stark,G.R. (1990). DNA amplification is rare in normal human cells. Proc Natl Acad Sci U S A *87*, 1791-5.

Xiao,Q., Claassen,G., Shi,J., Adachi,S., Sedivy,J., and Hann,S.R. (1998). Transactivation-defective c-MycS retains the ability to regulate proliferation and apoptosis. Genes Dev. *12*, 3803-3808.

APPENDIX-Abstracts

Abstract #1: Joon-Ho Sheen and Robert B. Dickson. Deregulated c-Myc alters DNA damage-dependent G1/S checkpoint. Georgetown University Medical Center and Lombardi Cancer Center Research Poster Day. Feburuary 2000.

Among the recently uncovered effects of c-Myc, genomic instability induced by this oncoprotein may provide one aspect of its oncogenic activity. Genomic instability in cancer cells, coupled with selective pressures, have been considered as driving forces for the accumulation of somatic mutations required for tumor progression. According to previous studies, overexpression of c-Myc induces genomic instability, including gene amplification and chromosomal instability. However, the molecular mechanism(s) for c-Myc-induced genomic instability has not been elucidated. Since abrogation of cell cycle checkpoint has been identified as a prerequisite in production of certain types of genomic instability, we studied the possibility that c-Myc alters checkpoint controls in response to DNA damage. Alteration of DNA damage-dependent checkpoint is thought to promote the accumulation of genetic damage in cells by allowing replication of unrepaired DNA damage in the following S phase. As a first step, to test this hypothesis, we investigated the DNA damage-dependent G1/S checkpoint, since c-Myc is well known to facilitate G1/S progression. In a flow cytometric study, HMEC (Human Mammary Epithelial Cells) and mouse fibroblast cells expressing deregulated c-Myc show a reduced proportion of G1/S arrested cells after γ-irradiation in contrast to the control parental cells. We also determined that both the MBI (Myc-Box I) and MBII (Myc-Box II) domains of c-Myc are required for the alteration of the G1/S checkpoint. These data suggest that transactivation of c-Myc target genes is required for the genetic destabilization effects of c-Myc. This ability of c-Myc to alter a crucial safeguard mechanism for genomic instability may therefore contribute to its role as a potent oncogene when its expression is deregulated. This work is supported in part by Department of the Army Fellowship grant # DAMD17-99-1-9205 to JHS.

Abstract #2: Joon-Ho Sheen and Robert B. Dickson. Deregulated c-Myc induces alteration of DNA damage-dependent G1/S checkpoint in human mammary epithelial cells. Abstract #2793. 91st Annual Meeting of American Association for Cancer Research. April 2000, San Francisco, CA.

Deregulated c-Myc has been implicated in breast cancer, both at the gene and protein levels. Among the recently uncovered effects of c-Myc, genomic instability induced by this oncoprotein may provide one aspect of its oncogenic activity. Genomic instability in cancer cells, coupled with selective pressures, have been considered as driving forces for the accumulation of somatic mutations required for tumor. According to previous studies, overexpression of c-Myc induces gene amplification and chromosomal instability. However, the molecular mechanism(s) for c-Myc-induced genomic instability has not been elucidated. Since abrogation of cell cycle checkpoint has been identified as a mechanism for certain types of genomic instability, we investigated the possibility of c-Myc-induced alteration in cell cycle arrest in response to DNA damage. Interestingly, according to flow cytometric study, HMEC (human mammary epithelial cells) with deregulated c-Myc show a significantly reduced proportion of G1/S-arrested cells after γ-irradiation. In contrast, the control HMEC, transfected with an empty vector, showed a large proportion of cells arrested at G1/S in response to DNA damage induced by γ-irradiation. These results suggest that c-Myc alters the DNA damage-dependent G1/S checkpoint. This alteration predisposes cells for the accumulation of genetic damage by allowing replication of unrepaired DNA damage in the following S phase. Previous studies of tumor suppressors such as p53 and pRB have shown abrogated checkpoint in the absence of the tumor suppressor. However, based on this study, we propose that activated oncogenes such as c-Myc may provide similar effects of altered checkpoint (supported by DOD Pre-doctoral grant to J.H.S.)

Abstract #3: Joon-Ho Sheen and Robert B. Dickson. 2001. Effects of c-Myc expression on G2/M arrest and aberrant mitosis following DNA damage. **In preparation.**

Effects of c-Myc overexpression were investigated on IR (ionizing radiation)-induced micronucleation and G2/M arrest, in human mammary epithelial cells (HMECs). We initially observed a dramatic increase, following γ-irradiation, in multiple micronuclei of MCF10A-MycER^{TM} cells, selectively following treatment with 4-OHT (4-hydroxy tamoxifen). Furthermore, these post-IR micronuclei contained newly synthesized DNA, according to a combination approach, using both γ-irradiation and BrdU treatment. Since formation of micronuclei is a post-mitotic event, tightly associated with genomic damage, this result indicates that damaged DNA managed to progress through both G1/S and G2/M checkpoints to form micronuclei. Similar results were obtained, consistently, in normal HMECs overexpressing c-Myc or p53DD (a dominant negative form of p53). Based on these results, we hypothesized that c-Myc attenuates the G2/M checkpoint and facilitates the entry of damaged DNA into M-phase, eventually leading to the formation of micronuclei in the post-M phase. To test this hypothesis, we employed a mitotic trapping assay to determine whether c-Myc attenuates the G2/M checkpoint. The MCF10A cells infected with an empty LXSN retroviral vector control or a c-MycS-containing retroviral vector did not show significant numbers of rounded-up cells (less than 1%) following prolonged post-IR incubation in the presence of nocodazole. In contrast, c-Myc- or p53DD-overexpressing cells, consistent with our hypothesis, demonstrated a significant percentage (roughly 10 % in each) of cells in mitosis, based on rounded cell morphology. Finally, we further examined the G2/M transition and mitotic progression following γ-irradiation, by using time-lapse videomicroscopy. After prolonged mitoses, following γ-irradiation, some cells eventually were observed to carry out 'unbalanced cytokineses'. The ultimate fate of those cells undergoing aberrant mitoses is currently not known; whether they undergo apoptosis or manage to survive with genomic alterations will require further study. Taken together, our results suggest that ionizing radiation induces micronucleation, possibly an indication of genetic alterations, through an altered G2/M transition and aberrant mitotic progression in c-Myc-overexpressing cells. Based on these findings, we propose that c-Myc overexpression induces checkpoint alterations, which contributes to the destabilization of cellular genome (supported by DOD Pre-doctoral grant # DAMD17-99-1-9205 to J.H.S.).

Abstract #4: Joon-Ho Sheen. July 2001. Effects of c-Myc expression on the DNA damage-induced cell cycle checkpoints. Ph.D. thesis dissertation, Department of Cell Biology, Georgetown University, Washington, DC.

Effects of c-Myc expression were investigated on the DNA damage-induced checkpoints at the G1/S and at the G2/M boundaries in human mammary epithelial cells (HMECs). We initially used flow cytometric analysis to identify a c-Myc-induced alteration of the G1/S checkpoint in two non-transformed HMEC lines - 184A1N4 and MCF10A. These results were confirmed using a BrdU incorporation assay, measuring *de novo* DNA synthesis. A transient excess of c-Myc activity, *via* the regulatable c-MycER, was, similarly, able to attenuate G1/S arrest, following ionizing radiation (IR). The c-Myc-induced G1/S alteration was also observed in finite lifespan, normal HMECs. In a molecular analysis, we observed deregulated hyperphosphorylation of Rb and then the reappearance of cyclin A, as the c-Myc-overexpressing cells entered into S phase, following IR. One additional finding from G1/S study is a dramatic increase in the cellular contents of multiple micronuclei, following IR, selectively in cells with excess c-Myc activity. Since micronucleation is a post-mitotic event, the results suggest a possibility of altered G2/M checkpoint by c-Myc. Therefore, we hypothesized that c-Myc alters the G2/M checkpoint, as well. We investigated the effects of c-Myc overexpression on the G2/M arrest following IR by employing a mitotic trapping assay, and obtained pilot data supporting our hypothesis. The MCF10A cells, overexpressing either c-Myc or dominant negative p53DD, demonstrated a significant percentage (roughly 10% in each) of cells in mitosis (based on rounded cell morphology), following prolonged post-IR incubation with nocodazole. In contrast, cells infected with an empty vector or a c-MycS-containing vector did not show significant numbers of rounded-up cells. Finally, mitoses of irradiated MCF10A-MycER cells were directly examined by time-lapse videomicroscopy. After prolonged mitoses, following IR, mitotic cells eventually were observed to carry out unbalanced cytokineses. Taken together, these results suggest that c-Myc alters safeguard mechanisms for genomic stability, both at the G1/S and at the G2/M boundaries. Alterations of the DNA damage-induced checkpoints, such as the one studied here, have been identified as crucial prerequisites for certain types of genomic instability, such as gene amplification. Therefore, based on these findings, we propose that deregulated c-Myc abrogates a safeguard mechanism(s) for genomic stability.

APPENDIX-Manuscript

Manuscript submitted: Joon-Ho Sheen and Robert B. Dickson. 2001. c-Myc alters the DNA damage-induced checkpoint at G1/S. **Submitted.**

- Copy of the Manuscript submitted Attached.

c-Myc alters the DNA damage-induced G1/S checkpoint

Joon-Ho Sheen and Robert B. Dickson*

Running title: c-Myc abrogates G1/S arrest

Departments of Oncology and Cell Biology, and Lombardi Cancer Center, Georgetown University Medical Center, Washington, D.C. 20007

*Corresponding author:

Dr. Robert B. Dickson

Room W417B, The Research Building,

Lombardi Cancer Center,

Georgetown University Medical Center,

3970 Reservoir Rd., N. W.,

Washington, DC 20007-2197.

Phone: (202) 687-3770.

Fax: (202) 687-7505.

E-mail: DicksonR@gunet.georgetown.edu

Abstract

Study of the mechanism(s) of c-Myc-induced genomic instability has the potential to shed new light on the genetic basis for the well-known oncogenic activity of this transcription factor. In the current study, the effect of c-Myc expression was investigated on the DNA damage-induced checkpoint at G1/S in human mammary epithelial cells (HMECs). We initially used flow cytometric analysis to identify a c-Myc-induced alteration of the G1/S checkpoint in two non-transformed HMEC lines - 184A1N4 and MCF10A. These results were then confirmed using a BrdU incorporation assay, measuring *de novo* DNA synthesis. A transient excess of c-Myc activity in MCF10A cells, using the regulatable MycER™, was similarly able to attenuate G1/S arrest following DNA damage. Importantly, the c-Myc-induced checkpoint alteration was also observed in finite lifespan, normal HMECs after transient expression of c-Myc from a retroviral construct. In our studies, we observed deregulated hyperphosphorylation of Rb and then the reappearance of cyclin A as the c-Myc-overexpressing cells entered into S phase following DNA damage. Alterations of the DNA damage-induced checkpoints, such as the one studied here, have been identified as crucial prerequisites for certain types of genomic instability, such as gene amplification. Therefore, based on these findings we propose that c-Myc abrogates a safeguard mechanism for genomic stability at the G1/S boundary; this property may contribute to the potent oncogenic activity of c-Myc.

Introduction

The c-*myc* oncogene has been implicated as a central switch in the onset or progression of many types of cancer. However, the underlying molecular mechanism(s) responsible for c-Myc-induced tumorigenesis remain elusive. Human c-Myc is a 439 amino acid protein, that when bound to its partner Max, can interact with DNA and function as a transcription factor. Myc-Max heterodimerization, which occurs through the interaction of C-terminal basic helix-loop-helix and leucine zipper motifs, is required for virtually all well-known c-Myc-associated phenotypes: cell proliferation, growth, transformation, and apoptosis (reviewed in (5;15;21). In addition to these well established phenotypes, recent studies have demonstrated that c-Myc expression can cause gross chromosomal aberrations and gene amplifications (22;43;44). The onset and progression of tumors depends upon the stepwise accumulation of somatic mutations in proto-oncogenes and tumor suppressor genes. Therefore, destabilizing genomic integrity may accelerate the accumulation of mutations required for the aggressive growth and malignant progression of tumors (8;37;42). As such, the c-Myc-induced genomic instability phenotype may provide an informative paradigm for understanding oncogene-induced tumor progression in general.

One mechanism crucial to the maintenance of genomic stability is that of the DNA damage-induced checkpoints (18;29;52;67). Cell cycle checkpoints ensure the proper execution of sequential events of the eukaryotic cell cycle; unprepared entry into either S phase or M phase can be fatal. As a cellular surveillance system for DNA

damage, the DNA damage-induced checkpoint is a specific class of cell cycle checkpoints that ensure that cells containing damaged DNA do not proceed into S phase or into mitosis (1;17;40;72).

Since a prominent role of c-Myc in the cell cycle is to facilitate G1/S progression, we have prioritized the G1/S checkpoint for our studies. Many biochemical components of the G1/S checkpoint have been identified, such as the tumor suppressor p53 and the CKI (cyclin-dependent kinase inhibitor) p21/Cip1 (cyclin-dependent kinase inhibitor protein 1) (27;71). When stabilized by a DNA damage signal, p53 is homotetramerized, and acts as a transcription factor. Among many downstream transcriptional targets of p53, p21/Cip1 has been identified as crucial for checkpoint controls; when its expression is upregulated, it arrests the cell cycle through inhibition of Cyclin/Cdk (cyclin/cyclin-dependent kinases) complexes. Thus, p21/Cip1 links p53 and the DNA damage-induced inhibition of cell cycle progression (17;19). These roles of p53 and p21/Cip1 in the DNA damage response are firmly established through recent studies using gene knock-out approaches (7;16;68;69). Inhibition of Cyclin/Cdk then leads to hypophosphorylation of the tumor suppressor Rb. The hypophosphorylated form of Rb proteins actively sequesters the E2F-1 transcription factor, preventing transactivation of E2F-1 targets. Since E2F-1-mediated transactivation is essential for progression into S phase, Rb-mediated inhibition of E2F-1 activity causes the cell cycle arrest at G1/S. The crucial involvement of Rb in the DNA damage-induced G1/S arrest was demonstrated in a study employing Rb (-/-) nullizygous mouse fibroblasts (28). Despite the appropriate upregulation of p53 and p21/Cip1 in Rb (-/-) fibroblasts

following DNA damage, the absence of Rb led to an abrogation of G1/S arrest.

Expression of c-Myc is highly regulated throughout the cell cycle (5), and deregulation of c-Myc leads to a shortened G1 and to a facilitation of G1/S progression (51). Therefore, we hypothesized that c-Myc overexpression may also override the scheduled cellular response (cell cycle arrest) to DNA damage at the G1/S boundary. In our studies of non-transformed, immortal HMEC lines and normal mortal HMECs, we demonstrated that c-Myc attenuates the G1/S arrest following ionizing radiation (IR)-induced DNA damage. For comparison, two independent controls were also used: an N-terminal truncated c-Myc (c-MycS) (60), and a dominant negative p53 (p53DD) (56). Furthermore, to demonstrate that a transient excess of c-Myc activity was sufficient to alter the G1/S checkpoint, we utilized a regulatable c-MycER^{TM} construct and transient expression of c-Myc *via* retroviral infection. Based on these findings, we suggest a model in which c-Myc can lead to an abrogation of a crucial safeguard mechanism for genomic stability in human mammary epithelial cells.

Materials and Methods

Cell culture

To study the effects of c-Myc overexpression in human mammary epithelial cells (HMECs), both immortal HMEC lines (184A1N4 and MCF10A) and normal mortal HMECs were used. The 184A1N4 clone (provided by Dr. M. Stampfer, Lawrence Berkeley National Laboratory and University of California, Berkeley, CA) was initially derived from an epithelial outgrowth of reduction mammoplasty tissue that was subjected to chemical immortalization, but not to malignant transformation (61;62). The 184A1N4-Myc line was originally established *via* retroviral transfection of 184A1N4 cells with a murine c-*myc* construct under the control of constitutively active MMLV (moloney mouse leukemia virus)-LTR (long terminal repeat) promoter (65). Both 184A1N4 and 184A1N4-Myc were maintained in Improved Minimal Essential Medium (IMEM; Life Technologies, Rockville, MD), supplemented with 0.5% fetal calf serum (FCS), 10 ng/ml epidermal growth factor (EGF), 5 μg/ml insulin, and 0.5 μg/ml hydrocortisone. The wild-type genomic sequences of *p53* genes in 184A1N4 and 184A1N4-Myc cells were confirmed by PCR sequencing of all exons at the Molecular Diagnostics Shared Resource of the Lombardi Cancer Center. MCF10A (obtained from the American Type Culture Collection (ATCC), Fairfax, VA) was originally derived from a s.c. mastectomy, performed on a 36-year old parous premenopausal woman; cells were immortalized spontaneously (59;64). MCF10A was maintained in 1:1 mixture of Dulbecco's Modified Eagle Medium (DMEM) and Nutrient Mixture F-12 medium

(DMEM:F-12; Life Technologies, Rockville, MD), supplemented with 5% horse serum, 20 ng/ml EGF, 10 μg/ml insulin, and 0.5 μg/ml hydrocortisone. Normal HMECs (#1001-8, CC-2551) at passage 8 were purchase from Clonetics-BioWhittaker, Inc. (Walkersville, MD), and cells between passage 8 and 10 were used for experiments. Normal HMECs were maintained according to the supplier's instructions in Mammary Epithelial Cell Growth Medium (MEGM, CC-3152), supplemented with 52 μg/ml Bovine Pituitary Extract, 10 ng/ml human EGF, 5 μg/ml insulin, and 0.5 μg/ml hydrocortisone. Normal HMECs were grown in 37°C incubators with low (0.1-0.2%) CO_2 settings.

Transgene constructs and retroviral infection

A full-length human *c-myc* cDNA construct, cloned in the pLXSN retroviral vector, was obtained from Drs. M. Stampfer and P. Yaswen (Lawrence Berkeley National Laboratory, Berkeley, CA). In pLXSN, transgene expression and polyadenylation are facilitated by a moloney murine sarcoma virus (MoMuSV)-long terminal repeat (LTR) promoter and a moloney murine leukemia virus (MoMuLV)-LTR polyadenylation signal (49). To create a retroviral construct expressing c-MycS, c-*myc* cDNA with a 5'-truncation was prepared through sequential recombinant DNA manipulations. Human *c-myc* cDNA has a unique recognition site for *Eco*RV between the first AUG (the second translation start codon) and the second AUG (Figure 2A), and pBluescript II-SK (+/−) possesses a unique *Eco*RV site which is immediately behind the *Eco*RI site in MCS (multiple cloning site) of the vector. Therefore, after the initial subcloning of human c-

myc cDNA into *Eco*RI site at MCS of the cloning vector, *Eco*RV fragments containing the 5′-truncated form of the human *c-myc* cDNA (c-*mycS*) were isolated by digesting the initial construct with *Eco*RV, and were then subcloned back into the *Hpa*I site in MCS of pLXSN retroviral vector by blunt-end ligation (Figure 2B). A subclone with *c-mycS* positioned in the correct direction was selected, and the predicted deletion of the 5′ region containing MB-I was confirmed by DNA sequencing. The pLXSN-*p53DD* (dominant negative p53) construct was provided by Dr. M. Oren (Weizmann Institute of Science, Israel). All cloning junctions in each construct were confirmed by DNA sequencing. For the preparation of a high-titer retrovirus stock, PA317 retroviral packaging cells were transfected with each construct, and G418 resistant high titer-producing clones were selected. To obtain stably transfected MCF10A pooled clones, cells were infected at a multiplicity of infection (MOI) of 5 in the presence of 8μg/ml polybrene twice sequentially in order to increase the viral copy number in the infected cells ((49), A. D. Miller, personal communication). After a week of drug selection with 200μg/ml G418, at least one thousand independent colonies were pooled together. The clones were pooled in order to overcome any effect of clonal variation and to examine the average effects of overexpression of transgenes. The pBabepuro-MycER™ constructs (encoding a fusion protein between N-terminal full-length human c-Myc and C-terminal engineered ligand-binding domain of a murine estrogen receptor; its inactive c-Myc conformation changes into an active c-Myc form when it binds to 4-hydroxy tamoxifen (4-OHT)) (24;39) were obtained from Drs. T. Littlewood (Imperial Cancer Research Fund, United Kingdom) and L. Z. Penn (University of Toronto,

Canada). MycER™ was subcloned into a LXSN vector in order to have all constructs in a single type of retroviral backbone, and LXSN-MycER™ was used to infect MCF10A for the isolation of single clones. For the transient expression of transgenes in normal HMECs, cells were infected at a MOI of 10 for 8-10 hrs in the presence of 8μg/ml polybrene. Cells were then grown for 24hrs to allow transgene expression, and then harvested for experimentation.

Cell proliferation assay

On Day 0, exponentially growing (~70% confluency) cells were harvested and plated on flat-bottom, 96-well plates (Becton Dickinson Labware, Franklin Lakes, NJ) at a density of 10^4 cells per well. After overnight attachment, the media was refreshed. For Day 1 (24hr) samples, immediately after media were refreshed, cells were washed two times with phosphate buffered saline (PBS), and stained for 15 min with 0.5% crystal violet solutions, containing 25% methanol as a fixative. After staining, cells were washed three times with tap water. Next, plates were allowed to air-dry. After the plates were dry, the stain was dissolved by adding 100μl of 0.1 M sodium citrate/50% ethanol, per well. The amount of stain was then quantitated and analyzed on *V*max kinetic microplate reader (Molecular Devices, Menlo Park, CA) at 570 nm, using the SOFTmax program. After the first media change on the Day 1, culture media were not further refreshed, in order to prevent any type of disturbance to the growing cells.

γ-Irradiation for inducing DNA damage

DNA damage was induced by IR treatment, using a ^{137}Cs source γ-irradiator (JL Shepherd Mark-I Irradiator, San Fernando, CA), at a rate of 3.6 Gray per minute, until the specified absorbed dosage was reached. For irradiation of attached cells in culture dishes, cells were plated, and irradiated on Day 2. For irradiation of suspended cells in conical flasks, each sample was adjusted to the same cell density (~3×10^6 cells per 5 ml culture medium in a 15 ml-conical tube). All experimental samples, either in dishes or in flasks, were kept rotating on the turntable inside the irradiator machine during the irradiation procedure.

Flow cytometric analysis of the cell cycle

For flow cytometric experiments to determine DNA content and the cell cycle profile, cells were plated at a density of 1-3 $\times$ 10^6 cells per T-75 flask. At the specified time points, cells were harvested, and fixed with ice-cold 100% ethanol while vortexing at low speed; cells were then placed at –20°C for overnight. After fixation, cells were centrifuged and washed once with PBS containing 1% BSA (bovine serum albumin). For staining with DNA dye, cells were resuspended in 0.5 -1ml of the propidium iodide solution containing RNase and incubated at 37°C for 30 min, followed by overnight incubation at 4°C. Cell cycle profiles were obtained using a FACScan flow cytometer (Becton Dickinson, San Jose, CA) and data were analyzed using MODFIT software.

BrdU labeling and immunofluorescence for *de novo* DNA synthesis

DNA synthesis was monitored by measuring incorporation of the artificial thymidine

nucleotide analog 5-bromo-2'-deoxy uridine (BrdU) (Sigma, St. Louis, MO) into newly synthesized DNA. After γ-irradiation, cells were plated on glass cover slips that were prewarmed in media in 12-well culture plates. 5×10^4 cells were plated per well and allowed, for the first 24 hrs, to grow in the complete media without BrdU. Next, cells were refreshed with complete media containing 10 μM (3 μg/ml) BrdU, and incubated for an additional 6 hrs or 24 hrs for BrdU incorporation. BrdU was added to the media from a 10,000× stock solution in distilled water. After BrdU incubation, cells were washed three times with PBS (10 min each wash) and fixed in 4% paraformaldehyde/PBS for 20 min. Next, the fixed cells were permeabilized with 0.5% Triton-X100/PBS. After the partial denaturation of DNA with 2N HCl, cells were incubated with a fluorescein-conjugated anti-BrdU mouse monoclonal antibody (Roche/Boehringer Mannheim, Indianapolis, IN), at 1:2 dilution (50 μg/ml) for one hour in the dark. Cells were then washed with PBS three times and counterstained with DNA dyes (propidium iodide (PI) or 4', 6'-diamidino-2-phenylindole (DAPI)) for 5 min. Finally, after several additional PBS washes, the cover clips were mounted on glass slides with Prolong mounting medium (Molecular Probes, Eugene, OR) for fluorescence microscopy. Quantitative analysis of immunofluorescence data was carried out with Image-Pro® Plus software (Media Cybernetics, Silver Spring, MD).

Western blot analysis

Cell lysates were prepared in 2× Laemmli sample buffer, containing 1% SDS and β-mercaptoethanol. After collecting approximately 10^6 cells in 100 μl of sample buffer,

whole cell lysates were boiled for 10 min, cleared by centrifugation at 4°C, and stored at –80°C until use. For SDS-polyacrylamide gel electrophoresis, 20 µl of the cleared lysates was loaded into a well of the gel. Separated proteins were transferred to Immobilon-P polyvinylidene fluoride membrane (Millipore, Bedford, MA). After tank transfer, membranes were blocked for 1 hr at room temperature in 0.05% Tween 20-PBS (PBS-T) containing 5% nonfat dried milk, and then probed with primary antibody diluted in PBS-T overnight in a 4°C cold room. Antibodies and concentrations were as follows; human c-Myc (9E10, 2µg/ml; 14851A Pharmingen, San Diego, CA), human p53 (PAb1801, 2.5µg/ml; Ab-2 Oncogene Research Products, Boston, MA), pan-species p53 (PAb 421, 10µg/ml; Ab-1 Oncogene Research Products), p21/WAF1 (EA10, 1µg/ml; Ab-1 Oncogene Research Products), human Rb (1µg/ml, 14001A Pharmingen), cyclin A (H-432, 1µg/ml; sc-751 Santa Cruz Biotechnology, Santa Cruz, CA), p14/ARF (1µg/ml; AHZ0472 Biosource, Camarillo, CA) and α-tubulin (DM1A, 1:1000 dilution; Ab-2 NeoMarkers, Fremont, CA). Blots were then washed with PBS-T three times for 10 min. All blots were next incubated in Horse Radish Peroxidase-conjugated secondary goat anti-mouse or anti-rabbit antibody (BioRad, 1:3000 dilution) for 1 hr at room temperature for chemiluminescent detection.

Hoechst staining for microscopic analysis of apoptosis

For the analysis of c-Myc-induced apoptosis with the MCF10A-MycER™ system, cells were starved of EGF for 6 days in the presence of ethanol (a vehicle control) or 1 µM 4-OHT. After harvest, cells were resuspended in 50 µl of PBS, and cell density was

checked under phase-contrast microscopy. Next, the entire population of resuspended cells was added to 350 µl of Hoechst staining solution consisting of 10 µg/ml Hoechst 33258 (B-2883 Sigma, St. Louis, MO), 1% NP-40, and 3.7% formaldehyde in PBS. Finally, the condensed nuclei of apoptotic cells were examined by fluorescent microscopy.

Results

c-Myc-overexpressing 184A1N4 HMECs exhibit an abrogation of G1/S arrest following IR-induced DNA damage

To determine if c-Myc overexpression alters the DNA damage-induced checkpoint at G1/S, we first investigated changes in cell cycle progression following irradiation of an isogenic pair of HMEC lines - 184A1N4 (hereafter termed A1N4) and 184A1N4-Myc (hereafter termed A1N4-Myc). The wild-type genomic sequences of *p53* genes in A1N4 and A1N4-Myc cells were confirmed by PCR-sequencing of all exons. We have chosen ionizing radiation (IR) as a DNA damaging agent because γ-irradiation can provide clearly defined effects of inducing DNA strand breaks. In order to determine the progression through the G1/S boundary, HMECs were first synchronized at G0/G1 phase by using EGF withdrawal technique. Previous studies with A1N4 and A1N4-Myc have demonstrated that EGF withdrawal technique allows a reversible G0/G1 synchronization (51). As expected, non-irradiated (0 Gray control) A1N4 and A1N4-Myc showed cell cycle progression and a gradual loss of synchrony during the 24hr post-IR incubation (roughly one cell cycle period of A1N4 and A1N4-Myc). In response to DNA damage induced by 6, 12, 24 Gray IR, respectively, 30%, 23.3%, 24% of A1N4 cells were arrested in G0/G1 phase (represented by 2N DNA content) and respectively, 52.2%, 55%, 52.7% of cells were located in G2/M phase (represented by 4N DNA content) (Figure 1). In A1N4-Myc cells, surprisingly, 42.2% of cells were located in G0/G1 and 51.7% of cells were in G2/M, following 6 Gray of IR.

However, only about ~3% of A1N4-Myc cells remained in G0/G1 phase, and most (89.3% in 12 Gray and 72.9% in 24 Gray) were located in G2/M phase following 12 and 24 Gray of IR. We interpreted these results to suggest that in response to DNA damage a significant percentage (~25-30%) of parental A1N4 cells arrested at the G1/S checkpoint. In contrast, a significant percentage (when compared to 12 Gray and 24 Gray profiles) of A1N4-Myc cells were able to repopulate G0/G1 following 6 Gray IR, and cells were arrested at G2/M only following 12 and 24 Gray IR. This result indicates that A1N4-Myc cells were altered for G1/S arrest following IR exposures of up to 24 Gray, and for G2/M arrest following IR exposures of up to 6 Gray. Furthermore, our data also suggested that the strength of the G1/S arrest signal correlates with the amount of DNA damage. Considering A1N4-Myc results, 24 Gray-induced DNA damage retarded the S-to-G2/M progression more severely (S phase percentage: 7.3% in 12 Gray- and 24.1% in 24 Gray-irradiated) than did 12 Gray-induced DNA damage.

Intact DNA damage-induced G1/S checkpoint in MCF10A HMECs and retroviral infection of the HMECs

In order to further examine the DNA damage-induced G1/S arrest in the background of an independently derived HMEC line, we tested the response of MCF10A to IR-induced DNA damage; MCF10A cells have been well documented to have wild-type, functional p53 (25;47). For MCF10A and later studies, we irradiated an actively growing, asynchronous population of MCF10A cells. This design was chosen in order to avoid complications resulting from repeated EGF withdrawal and stimulation.

Also, we measured changes in S phase fraction following IR as an indicator of the amount of cells entering into S through G1/S checkpoint. In comparison to the G0/G1 fraction, which is complicated by potential entries from the G2/M fraction, the S-phase fraction provided a measurement of the number of cells that had traversed the G1/S checkpoint. However, since this S fraction measurement still did not include S phase cells that exited to G2/M, this parameter is likely to provide a minimal estimate of G1/S passage. To corroborate these data, we next employed an assay of BrdU incorporation, measuring *de novo* DNA synthesis and representing all cells encountering S phase. According to the flow cytometric profile, MCF10A cells were obviously arrested at both G1 and G2/M phases following IR of 4 to 12 Gray, with a significant reduction in S phase fraction (data not shown). These data clearly demonstrated that parental MCF10A cells retain an intact G1/S checkpoint. Based on these results we have chosen 12 Gray of IR to induce DNA damage in all of our subsequent experiments.

We next introduced a human *c-myc* cDNA construct (Figure 2A) into MCF10A cells and into NIH3T3 mouse fibroblasts (as an additional control). In addition to the full-length *c-myc*, we also employed two independent controls; an N-terminal truncated *c-myc* (*c-mycS*) and a dominant negative *p53* (*p53DD*) (Figure 2B). c-MycS is known to be defective in c-Myc-induced transactivation (60), and as such served as an additional negative control, together with the empty vector control. p53DD (3;56) served as a positive control for this study by providing an abrogated checkpoint phenotype in HMECs. After MCF10A cells were infected with the empty vector, human *c-myc*, *c-mycS*, or murine *p53DD* construct, we pooled all G418-resistant colonies from each

infection procedure and examined the expression of each exogenous gene. For the full-length c-Myc, use of the anti-human Myc antibody 9E10 did not distinguish the exogenous human c-Myc from the endogenous protein (Figure 2C). Although the endogenous expression of human c-Myc was tightly regulated upon the cell cycle progression, c-Myc was detected at a relatively significant level in exponentially growing MCF10A-LXSN (MCF10A cells infected with empty LXSN vector only). Therefore, we also infected the mouse embryonic fibroblast line, NIH3T3, with the same retroviruses and confirmed the expression of the exogenous human c-Myc in this system. As predicted, cells infected with human *c-mycS* showed only the overexpression of a 46kDa protein, a truncated version of human c-Myc. In MCF10A-Myc (MCF10A cells infected with human *c-myc*), the level of c-Myc was elevated to a level of about 2- to 3-fold compared to that of the MCF10A-LXSN control. However, since it is known that c-Myc down regulates its own expression through an autorepression mechanism (20), we believe that majority of the signal is due to expression of the introduced exogenous gene (53). In addition, the constitutive overexpression of exogenous c-Myc was evident following γ-irradiation (Figure 4). Expression of p53DD was also confirmed by western analysis. Importantly, the overexpression of murine p53DD stabilized the endogenous human p53 (Figure 2D). This served as verification that the murine p53DD proteins could bind to the endogenous human p53 protein to inhibit its function. Heterooligomer formation between the p53DD and the full-length p53 is thought to impair the scheduled degradation of endogenous p53 and to lengthen its half-life (56). The level of p21/Cip1 was also low in the MCF10A-p53DD, indicating that the

increased amount of p53 proteins in these cells is not functional (Figure 2D).

To confirm the pro-proliferation activity of c-Myc, we performed a 96-well plate proliferation assay (Figure 2E). Although, on Day 0, we plated exponentially growing (~70% confluency) cells on the 96-well plates, it appeared that the initial population doubling time (PDT) is much longer than the later PDT. Since we usually plated the exponentially growing cells on the day before experiments, the initial PDT was more relevant for most experiments. The estimated initial PDTs (based on a 48hr to 72hr period) are: 31.4hr for MCF10A-LXSN, 20.4hr for MCF10A-Myc, 32.2hr for MCF10A-MycS, and 27.6hr for MCF10A-p53DD. The growth rate of MCF10A-Myc was the fastest; this is consistent with pro-proliferation effects of c-Myc. The growth rate of MCF10A-MycS was slower than that of MCF10A-LXSN. MCF10A-p53DD cells grew at a rate marginally faster to that of the MCF10A-LXSN control population. Thus, abrogation of p53 did not provide a significant acceleration for the proliferation of MCF10A cells growing *in vitro*.

c-Myc attenuates G1/S arrest following IR-induced DNA damage in MCF10A HMEC

MCF10A HMECs harboring the aforementioned transgenes were irradiated in suspension, and were then replated in culture flasks. After 24 hrs or 48 hrs of post-IR incubation, cell cycle profiles and S fractions were analyzed by flow cytometry. Representative flow cytometric data (Figure 3A) of MCF10A-LXSN showed that 12 Gray of IR induced a dramatic decrease in S-phase fraction (58.5% $_{\text{S-reduction}}$ in post-24hr and 78.0% $_{\text{S-reduction}}$ in post-48hr) when compared to the non-irradiated control (% s-

$_{\text{reduction}}$ = (% $_{\text{S in non-irradiated}}$ - % $_{\text{S in irradiated sample}}$) / % $_{\text{S in non-irradiated}}$). This IR-induced reduction of S phase is similar (57.4% $_{\text{S-reduction}}$ in post-24hr and 82.1% $_{\text{S-reduction}}$ in post-48hr) in MCF10A-MycS. In contrast, although MCF10A-Myc results seem similar (56.3% $_{\text{S-reduction}}$) in post-24hr to the MCF10A-LXSN and MCF10A-MycS, they showed a significant percentage of cells located in S phase after 48 hrs post-IR (57.9% $_{\text{S-reduction}}$ in post-48hr). As expected, MCF10A-p53DD showed an abrogated checkpoint phenotype (10.3% $_{\text{S-reduction}}$ in post-24hr and 26.4% $_{\text{S-reduction}}$ in post-48hr). IR also induced a moderately lower percentage of cells in G0/G1 (2N complement) in c-Myc- or p53DD-infected cells, compared with LXSN- or c-MycS-infected cells (percentage of G0/G1: LXSN 74.3%, Myc 61.1%, MycS 72.7%, and p53DD 39.0%) in 48hr post-IR results. In independently repeated flow cytometric assays, the overall patterns were consistent; c-Myc- or p53DD-infected MCF10A cells maintained a higher S fraction and a moderately lower G0/G1 fraction, compared to controls, following γ-irradiation.

In order to confirm this c-Myc-induced alteration of G1/S checkpoint, we performed BrdU incorporation assays for *de novo* DNA synthesis. Following IR treatment of each infected MCF10A population, the immunofluorescence results were consistent with the flow cytometric data (Figure 3B). After IR, cells were pre-incubated for 24 hrs before adding BrdU. This initial 24hr post-IR incubation allowed a sufficient time for S phase cells to exit S phase to the next phase. Next, the culture media were changed to BrdU-containing complete media, and cells were incubated for an additional 24 hrs for BrdU incorporation. In all four groups of sample populations, although a significant period of BrdU incubation was allowed, non-irradiated controls failed to

exhibit 100% saturation of BrdU incorporation (LXSN 45.4%, c-Myc 53.2%, c-MycS 50.7%, and p53DD 54.8%). However, MCF10A-LXSN showed a dramatic loss of BrdU labeling (to 4.9%) following 12 Gray of IR (Figure 3B). MCF10A-MycS also demonstrated a significant loss of BrdU labeled cells (to 1.5%), which is consistent with flow cytometric results. In contrast, both c-Myc- and p53DD-infected MCF10A showed a higher frequency of BrdU incorporation; 29.2% in c-Myc-infected and 46.8% in p53DD-infected cells. We concluded, taking all of these data together, that deregulated c-Myc attenuated G1/S arrest following DNA damage in HMECs.

c-Myc-induced alteration of the G1/S checkpoint accompanies the deregulated hyperphosphorylation of Rb and reappearance of cyclin A

To gain further insight into the underlying molecular basis of the c-Myc-induce G1/S checkpoint alteration, we analyzed the levels of several cell cycle related proteins in a time course. First, we started with c-Myc itself. Interestingly, the oncoprotein itself was downregulated in the LXSN-, c-MycS-, or p53DD-infected MCF10A cells following IR (Figure 4A). The reduction of c-Myc was significant in as early as 18hr post-IR sampling in all three populations. However, the level of c-Myc was maintained relatively high and unaffected by IR treatment in MCF10A-Myc. Reprobing the same blot with an anti-Rb antibody demonstrated deregulated hyperphosphorylation of Rb only in c-Myc- or p53DD-infected cells. Since we irradiated exponentially growing, asynchronous HMECs, various levels of phosphorylation in Rb were detected at the 0 hr time-point. However, the majority of hyperphosphorylated Rb (ppRB) disappeared

as early as 5hr post-IR, in all sample groups. The hypophosphorylated Rb (pRB) dominated until 24hr post-IR in LXSN- or c-MycS-infected cells. In contrast, c-Myc- or p53DD-infected cells showed a rapid reappearance of hyperphosphorylated Rb (slower migrating bands) as early as 18hr post-IR. Rb is a prominent target for Cdk2-cyclin E and Cdk2-cyclin A during scheduled G1/S progression, and we wanted to assess any changes of Cdk2 holoenzyme status after DNA damage. Cyclin A and/or cyclin E are well-established, positive regulatory subunits for Cdk2; the levels of cyclins mainly determine the activities of Cdk holoenzymes. In our results, cyclin A was dramatically suppressed after 18hr post-IR in the LXSN- or c-MycS-infected cells. However, cyclin A reappeared, up to the previous level, after 24hr post-IR in the c-Myc- or p53DD-infected cells. Since the level of cyclin A is also high in S phase cells, this result further supports the conclusion that c-Myc alters the G1/S checkpoint and allows unprepared entry into S phase after DNA damage.

To test the p53-dependent response following IR, we performed a time-course western blot analysis of p53 and its downstream effector p21/Cip1. As expected, the endogenous p53 protein was upregulated in MCF10A-LXSN, MCF10A-Myc, and MCF10A-MycS in 3hr post-IR time point. Stabilized, but non-functional, endogenous full-length p53 in MCF10A-p53DD was also apparent. Next, upregulation of p21/Cip1 appeared as early as 6hr post-IR time point, following the upregulation of p53. The c-Myc partner, Max is known to maintain a constant protein level throughout the cell cycle; it served a loading control in the western analysis.

Transient excess of c-Myc activity is sufficient to induce G1/S checkpoint alteration

In the checkpoint experiments for MCF10A HMEC, we pooled the transfected MCF10A colonies following drug selection to provide an average phenotype in the absence of clonal variations. However, it has been demonstrated in a fibroblast model that deregulated c-Myc activity can induce various genomic instabilities in a reasonably short-term period (22). Therefore, it was necessary to determine whether the previously shown G1/S alteration phenotype is due to secondary genetic alterations acquired during the drug selection period. To address this question, we established a regulatable Myc system with MCF10A. c-MycER™ is a fusion protein consisting of full-length human c-Myc (at the N-terminus) and hormone-binding domain of murine estrogen receptor (ER) (at the C-terminus). Only in the presence of an ER-binding ligand, such as 4-hydroxytamoxifen (4-OHT), does the C-terminal hormone-binding domain fail to interfere with the function of N-terminal c-Myc, enabling the activation of c-Myc in a post-translational manner. First, we confirmed the expression of MycER™ in MCF10A HMECs at the expected size of 110 Kd. Next, we demonstrated that 4-OHT treatment downregulated the endogenous c-Myc, in comparison to the EtOH vehicle treatment. This is consistent with negative feedback regulation at the c-*myc* promoter (Figure 5A).

For the confirmation of a functional MCF10A-MycER™ system, we observed phase-contrast images of cellular apoptosis induced by c-Myc; a Hoechst 33258 dye assay was to identify apoptotic nuclei. c-Myc is well known to induce apoptosis, particularly in the absence of growth/survival factors. Therefore, we starved cells of EGF (Epithermal Growth Factor) for up to 6 days, in the presence of EtOH or 4-OHT

(Figure 5B). After 4 days of this treatment, the morphological difference between EtOH-treated cells and 4-OHT-treated cells was identifiable. In comparison to the flattened cellular morphology with EtOH/-EGF treatment, 4-OHT/-EGF treatment induced a slender cellular morphology (see the yellow arrows in Figure 5B) and significant amounts of floating bodies. In the Hoechst 33258 dye staining, we could identify the fragmented and condensed apoptotic nuclei (see the yellow arrows in Figure 5C), selectively in 4-OHT-stimulated MCF10A-MycER™ cells (~3% of roughly 400 nuclei observed in samples of 4-OHT/-EGF treated cells) (Figure 5C and 5D). Therefore, we concluded that c-Myc activity could be regulated by 4-OHT in MCF10A-MycER™ system.

To test if the transient excess of c-Myc activity is sufficient to abrogate the DNA damage-induced G1/S arrest, we repeated the previously-described scheme of our BrdU incorporation following 0 or 12 Gray of IR (Figure 6). In the absence of IR-induced DNA damage, 4-OHT-treated MycER™ cells showed a higher BrdU incorporation (37.1%) than that of the EtOH vehicle-treated ones (33.6%). In 12 Gray-irradiated MCF10A-MycER™ cells, only those stimulated with 4-OHT demonstrated a suppressed, but significant amount (28.2%) of BrdU-labeled nuclei, consistent with results of the permanently transfected MCF10A. Furthermore, significant amounts of multi-micronucleated nuclei, displaying BrdU incorporation, were selectively identified in γ-irradiated cells. These BrdU-labeled nuclei had morphologies distinct from the condensed apoptotic nuclei. Therefore, it is unlikely that the BrdU incorporation occurred as a part of the apoptosis process in HMECs with deregulated c-Myc.

c-Myc alters the DNA damage induced G1/S checkpoint in normal HMECs with a finite lifespan.

One of the important questions about the DNA damage-induced checkpoint control is whether a specific genetic alteration (such as activation of c-*myc* in this study) is able to alter the checkpoint in normal human cells with a finite lifespan. Establishment of immortalized cells from mortal primary human cells may involve genetic mutations in known and/or unknown genes, complicating interpretation of checkpoint control studies. Therefore, we needed to investigate whether overexpressed c-Myc is able to attenuate G1/S arrest in normal HMECs with a finite lifespan. First, we checked expression of transgenes in normal HMECs after transient retroviral infection (Figure 7A). Following 48 hr post-infection (without drug selection), elevated levels of c-Myc or c-MycS could be identified in c-Myc- or c-MycS-infected normal HMECs. Similarly, p53DD-infected cells demonstrated stabilization of the endogenous p53, accompanied by a decreased amount of p21/Cip1. c-Myc-infected HMECs also showed a slightly increased level of p53 and of p14/ARF, known transcriptional targets of c-Myc in some cell types.

We next studied the response of normal HMECs transiently overexpressing c-Myc to IR-induced DNA damage. In this study, we irradiated retrovirus infected cells with 0 Gray or 12 Gray IR, and then observed morphological changes following 48 hrs of post-IR incubation under phase contrast microscopy (Figure 7B). Flattened cellular morphologies were apparent in non-infected (None) and c-MycS-infected HMECs.

However, following γ-irradiation and prolonged incubation, c-Myc- or p53DD-infected cells frequently demonstrated rounded-up or floating bodies. We next repeated the same experimental scheme for BrdU incorporation, as previously described for MCF10A cells. For normal HMECs, we employed a 6-hr BrdU pulse, instead of a 24 hr-BrdU incubation in order to avoid potential complications resulting from a prolonged incubation with BrdU. Though we consider it unlikely, we felt it necessary to rule out a possibility that the observed BrdU incorporation might result from apoptosis. After 34 hrs of post-infection and following 24 hrs of post-IR incubation, we refreshed the culture media with BrdU-supplemented media and further incubated cells for additional 6 hrs. All four non-irradiated groups of samples exhibited significant incorporations of BrdU after 6-hr BrdU pulse (None 21.3%, c-Myc 33.5%, c-MycS 25.4%, and p53DD 57.7%) (Figure 7C). However, non-infected (None) or c-Myc-S-infected cells showed an obvious loss of BrdU incorporation (4.6% in None and 5.6% in c-MycS) following 12 Gray of IR. In contrast, either c-Myc- or p53DD-infected MCF10A cells demonstrated significant BrdU incorporations; 26.1% in c-Myc-infected and 30.5% in p53DD-infected cells.

Discussion

c-Myc-induced genomic instability and checkpoint alteration

c-Myc induces aneuploidy, polyploidy, and gene amplifications in cultured fibroblasts (22;43;44). Previously, in mouse mammary carcinoma cells derived from *c-*

myc-transgenic mice, our group also identified chromosome translocations, trisomy, and dicentric chromosomes (41;45;70). To initiate our study of underlying molecular mechanism(s) of c-Myc-induced genomic instability, we examined DNA damage-induced G1/S arrest in HMECs overexpressing c-Myc. As briefly described in the Introduction, checkpoint(s) represent a critical safeguard mechanism(s) for the tightly coordinated progression of the cell cycle; they protect genomic stability through the prevention of unprepared DNA synthesis and DNA segregation (2;14;33). By employing flow cytometry-based cell cycle analysis and BrdU-incorporation assays, we have found that c-Myc expression attenuates the DNA damage-induced G1/S arrest, both in immortal HMEC lines and in mortal normal HMECs.

One consideration for the interpretation of our BrdU assay results might be that BrdU could additionally incorporate into the damaged chromosomes during DNA repair. However, it is thought that the level of BrdU incorporation due to DNA repair is miniscule compared to the level of BrdU incorporation caused by replicative DNA synthesis. In addition, it is unlikely that only c-Myc- or p53DD-infected cells undergo a massive DNA repair following the same dosage of IR. We also considered the possibility that this G1/S alteration is caused by sporadic mutations occurring during the preparation of retrovirus-infected cells. However, the G1/S checkpoint was examined at early passage after pooling thousands of drug-resistant colonies in retrovirus-infected MCF10A cells. Furthermore, we utilized the MycER™, a regulatable c-Myc construct, in order to demonstrate that the transient excess of c-Myc activity was sufficient to alter the G1/S checkpoint. In this regulatable system, we directly

demonstrated the effects of c-Myc on checkpoint controls, clearly ruling out the possibility of secondary genetic alterations in this process. Finally, this phenotype was confirmed in transiently infected normal HMECs. Taken together, these results suggest the possibility that c-Myc-induced checkpoint alterations precede oncogene-induced genomic instability. Therefore, future studies may productively employ time course experiments to dissect the problem of genomic instability and checkpoint abrogation in the regulatable c-Myc system.

A caveat for study of checkpoint phenotypes in immortalized cell lines is that observed alterations could be due to mutations acquired during the immortalization process or during repeated passaging of the cells. It has been shown that the vast majority (reportedly ~80%) of rare, immortal mouse embryonic fibroblasts (MEFs) are hypo-tetraploid and harbor mutant p53 alleles. Those that remain near-diploid frequently sustain biallelic loss of the p19/*ARF* locus (the mouse homolog of human p14/ARF) (58). According to the recent studies of p19/ARF (-/-) nullizygous MEFs, loss of p19/ARF alters the DNA damage-induced G1/S arrest (32), supporting the importance of p19/ARF in constituting a fully functional G1/S checkpoint in MEF system. These findings raise valid concerns about using immortal mouse cell lines for such studies. However, the situation with human mammary epithelial cell cultures appears to be different. Contrasted to fibroblasts, HMECs exhibited a more extended proliferative potential, and neither the elimination of p53 or p14/ARF are necessary for their immortalization (35). However, to rule out the contributions from unknown immortalizing mutations, we decided to re-confirm the effects of c-Myc overexpression

in non-immortalized normal human cells, and repeated our studies in normal HMECs (Figure 7). According to a previous report on the checkpoints of HMECs (48), both immortal and mortal HMECs demonstrated a lack of G1/S arrest following 4 Gray IR-induced DNA damage. Consistent with this previous report, we also identified an attenuated G1/S arrest following low doses (4 Gray) of IR (data not shown) in parental normal HMECs. However, following 12 Gray IR, a difference between parental HMECs and c-Myc-overexpressing HMECs was clearly identified (Figure 7C and 7D). Taken together, our results strongly suggest that either activation of c-Myc or inactivation of p53 is sufficient to attenuate G1/S arrest following IR-induced DNA damage in HMECs.

Previous studies have addressed a similar role of c-Myc in the abrogation of PALA (N-phosphonoacetyl-L-aspartate)-induced G1/S arrest (10;22). PALA, a chemotherapeutic drug, is a competitive inhibitor for CAD (carbarmyl phosphate synthase, aspartate transcarbamylase, and dihydroorotase), a trifunctional enzyme essential for pyrimidine synthesis. In PALA-treated normal cells, nucleotide synthesis is disrupted, resulting in an unbalanced nucleotide pool, and subsequent G1/S arrest. These previously published results inferred a potential role for c-Myc in the abrogation of DNA damage-induced checkpoint(s), by virtue of the putative ability of PALA to induce DNA damage and lead to DNA damage-induced checkpoint response. However, this interpretation is complicated by the fact that it was not clear whether the disturbed nucleotide pool *or* the resulting DNA damage induced cell cycle arrest. Importantly, it has been demonstrated that c-Myc-induced override of p53-dependent

cell cycle checkpoint is not restricted to DNA damage-induced G1/S arrest. Li and Dang (38) recently reported the effects of c-Myc overexpression on the post-M spindle assembly checkpoint, which responds to mitotic spindle damage and arrests cells at a post-M phase with 4N DNA content (14). This post-M spindle assembly checkpoint was originally identified as a p53-dependent checkpoint, because of its abrogation in p53 (–/–) or p21/Cip1 (–/–) nullizygous cells (14;33;36;63). However, after treatment of cells with nocodazole, only c-Myc-overexpressing HMECs exhibited octaploidy (8N). This observation has been independently reproduced in our group (J.H. Sheen and R. B. Dickson, unpublished data). Therefore, it would be interesting to determine whether this phenotype is mechanistically related to the altered G1/S checkpoint phenotype demonstrated here.

Micronulei formation following prolonged post-IR incubation

An unexpected, intriguing finding of the current G1/S study is a significant amount of micronuclei formation following prolonged incubation after γ-irradiation, especially in results with the transient excess of c-Myc activity (Figure 6). According to the previous study of c-Myc-overexpressing rat embryonic cells (REC:Myc) by using the computerized video time lapse (CVTL) methodology (23;66), REC:Myc cells were observed to be susceptible to IR-induced apoptosis after 4 - 9.5 Gray of IR. Cell death primarily occurred by postmitotic apoptosis following several divisions of the irradiated cells. Therefore, although the response of parental REC was not clearly described, these results might suggest the possibility of an abrogated G2/M entry

checkpoint, because the c-Myc-overexpressing REC were allowed to undergo several mitotic divisions, following IR treatment. Additionally, previous studies by McKenna et al. (46) reported a minimal delay in G2/M of Myc-expressing fibroblast following IR. In comparison to Myc/Ras-expressing fibroblasts, that display an extended delay in G2/M, c-Myc-expressing fibroblasts were more susceptible to IR-induced apoptosis. IR-induced apoptosis in this model was distinct from c-Myc-induced apoptosis in the absence of growth/survival factors. Therefore, these studies provide an interesting clue to initiate more rigorous investigation of the role of deregulated c-Myc in the DNA damage-induced G2/M checkpoint. Supporting this hypothesis, we have already demonstrated that a significant amount of A1N4-Myc cells did not arrest at G2/M, following a low dose (6 Gray) of IR, compared to their arrest at G2/M, following a high dose (12 or 24 Gray) of IR (Figure 1). Furthermore, the CVTL study reported that 60% of the progeny of 4 Gray IR-irradiated REC:Myc either had micronuclei or were sisters of cells having micronuclei. The formation of micronuclei was correlated to apoptosis, as cells with micronuclei were more likely to undergo apoptosis during the generation in which the micronuclei were observed (23;66). Therefore, it might be interesting to further characterize these cell-derived entities with rounded-up morphology, following 6 to 12 Gray of IR (data not shown for MCF10A, and Figure 7B for normal HMEC) and the BrdU-positive cells with micronuclei, after 12 Gray of IR (Figure 6). If HMECs respond to the G2/M checkpoint in a fashion similar to the above described, altered G1/S progression following DNA damage may precede massive, IR-induced, postmitotic apoptosis.

How does c-Myc override the p53-dependent pathway? Downstream targets for the c-Myc-induced checkpoint alteration

Since its discovery, some 20 years ago, c-Myc has been one of the most paradoxical oncogenes. It is well known that c-Myc facilitates two very important, but as yet seemingly opposite effects on cells; proliferation and apoptosis. The c-Myc-induced checkpoint alteration phenotype is not exempt from this type of paradox. p53 and ARF, two recently uncovered transcriptional targets of c-Myc, make c-Myc's action on the cell cycle even more intriguing. As described previously, checkpoint control has been extensively studied, in terms of p53 and its downstream targets, such as p21 for G1/S, and 14-3-3σ for G2/M (1;9;16;17;19;30;68). Interestingly, p53 and ARF were reported to be transactivated by c-Myc in some cell types (55;73). ARF inhibits the MDM2-mediated degradation of p53, resulting in stabilization of p53 (57). Although a significant increase of p53 protein was not detected following c-Myc infection of MCF10A, an IR-induced upregulation of p53 and p21/Cip1 protein was confirmed, both in LXSN- and in c-Myc-infected HMECs, over the same time-course (Figure 4B). According to several independent reports, c-Myc transrepresses p21, a universal Cdk inhibitor (11;12;50). Since p21 is a critical downstream effector of p53-mediated G1/S arrest, it would be a plausible target for c-Myc-induced override of this G1/S checkpoint. Our results however demonstrate only a subtle decrease of p21/Cip1 proteins in c-Myc-infected cells, following its initial upregulation at 6hr post-IR (Figure 4B). Therefore, further molecular analyses following IR-induced DNA damage are

needed to address the possible role of p21/Cip1 in the c-Myc-induced alteration of G1/S checkpoint.

Another candidate downstream target of c-Myc for override of the G1/S checkpoint could be Rb, the retinoblastoma protein. Rb is a major downstream effector of the p53-p21-Rb pathway for DNA damage-induced G1/S arrest. According to previous studies, the absence of Rb in the Rb (−/−) nullizygous MEFs leads to an inappropriate entry into the S-phase, following IR treatment (28). The rapid reappearance of hyperphosphorylated Rb in c-Myc-infected cells, following IR, suggests the participation of Rb in c-Myc-induced G1/S checkpoint alteration. However, because cells inactivate Rb through hyperphosphorylation when they enter into S, it is not clear yet whether c-Myc directly targets Rb-phosphorylation or whether this effect is just a result of unscheduled entry into S. The hyperphosphorylation of Rb, following IR, is also detected in p53DD-infected cells. The inappropriate hyperphosphorylation of Rb coincided with the reappearance of cyclin A, both in c-Myc-infected and in p53DD-infected populations. Expression of cyclin A is likely to have returned coincident with c-Myc- or p53DD-infected cells progressing again into S phase, even after IR. Cyclin A is known to be a major cyclin for regulation of S phase. Any possible change of cyclin E levels, following IR, has not yet been determined. Reportedly, c-Myc transactivates cyclin E, and this results in deregulated activation of Cdk2-cyclin E and hyperphosphorylation of Rb (4;26;31;54). As an interesting alternative approach for uncovering mechanisms of c-Myc-induced hyperphosphorylation of Rb would be to carry out a study of differential phosphorylation of Rb, following IR (6). The

retinoblastoma protein has 16 potential phosphorylation sites. Cdk4-cyclin D and Cdk2-cyclin A/E differentially, although not selectively, phosphorylate these sites of Rb (13;34). Therefore, a time-course study of site-specific phosphorylation of Rb, following IR, may provide interesting clues for determining a major cyclin-dependent kinase involved in the c-Myc-induced S entry after DNA damage.

Based on the current study, we propose that c-Myc alters the DNA damage-induced G1/S checkpoint, a molecular safeguard mechanism for genomic stability. This effect of c-Myc may contribute to its role as a potent oncogene. It will be interesting for future studies to address how c-Myc overrides p53-dependent arrest following IR-induced DNA damage, and what is the fate of c-Myc-overexpressing HMECs that have undergone replication of damaged DNA.

Acknowledgements

We thank Dr. Todd Waldman for much help throughout this study. We also thank Drs. T. Littlewood, A. D. Miller, M. Oren, L. Z. Penn, M. Stampfer, and P. Yaswen for the materials and advice, and are grateful for technical assistance from the FACS core, the microscopic imaging core, and the molecular diagnostics core facilities at the Lombardi Cancer Center in Georgetown University Medical Center. We thank Dr. Tim Jorgensen and members of our laboratory for comments on this manuscript. This study was supported in part by a pre-doctoral training grant of DOD breast cancer research program (DAMD17-99-1-9205) to JHS and NIH R01AG1496 to RBD.

References

1 **Agarwal, M. L., A. Agarwal, W. R. Taylor, and G. R. Stark**. 1995. p53 controls both the G2/M and the G1 cell cycle checkpoints and mediates reversible growth arrest in human fibroblasts. Proc Natl Acad Sci U S A **92**:8493-7.

2 **Almasan, A., S. P. Linke, T. G. Paulson, L. C. Huang, and G. M. Wahl**. 1995. Genetic instability as a consequence of inappropriate entry into and progression through S-phase. Cancer Metastasis Rev **14**:59-73.

3 **Bacus, S. S., Y. Yarden, M. Oren, D. M. Chin, L. Lyass, C. R. Zelnick, A. Kazarov, W. Toyofuku, J. Gray-Bablin, R. R. Beerli, N. E. Hynes, M. Nikiforov, R. Haffner, A. Gudkov, and K. Keyomarsi**. 1996. Neu differentiation factor (Heregulin) activates a p53-dependent pathway in cancer cells. Oncogene **12**:2535-2547.

4 **Berns, K., E. M. Hijmans, and R. Bernards**. 1997. Repression of c-Myc responsive genes in cycling cells causes G1 arrest through reduction of cyclin E/CDK2 kinase activity. Oncogene **15**:1347-1356.

5 **Blackwood, E. M., B. Luscher, L. Kretzner, and R. N. Eisenman**. 1991. The Myc:Max protein complex and cell growth regulation. Cold Spring Harb Symp Quant Biol **56**:109-117.

6 **Brugarolas, J., K. Moberg, S. D. Boyd, Y. Taya, T. Jacks, and J. A. Lees**. 1999. Inhibition of cyclin-dependent kinase 2 by p21 is necessary for retinoblastoma protein-mediated G1 arrest after gamma-irradiation. Proc Natl Acad Sci U S A **96**:1002-1007.

7 **Bunz, F., A. Dutriaux, C. Lengauer, T. Waldman, S. Zhou, J. P. Brown, J. M. Sedivy, K. W. Kinzler, and B. Vogelstein** . 1998. Requirement for p53 and p21 to sustain G2 arrest after DNA damage. Science **282**:1497-1501.

8 **Cahill, D. P., K. W. Kinzler, B. Vogelstein, and C. Lengauer**. 1999. Genetic instability and darwinian selection in tumours. Trends Cell Biol **9**:M57-M60.

9 **Chan, T. A., H. Hermeking, C. Lengauer, K. W. Kinzler, and B. Vogelstein**. 1999. 14-3-3Sigma is required to prevent mitotic catastrophe after DNA damage. Nature **401**:616-620.

10 **Chernova, O. B., M. V. Chernov, Y. Ishizaka, M. L. Agarwal, and G. R. Stark**. 1998. MYC abrogates p53-mediated cell cycle arrest in N-(phosphonacetyl)-L-aspartate-treated cells, permitting CAD gene amplification. Mol Cell Biol **18**:536-45.

11 **Claassen, G. F. and S. R. Hann**. 2000. A role for transcriptional repression of p21CIP1 by c-Myc in overcoming transforming growth factor beta -induced cell-cycle arrest. Proc.Natl.Acad.Sci.U.S.A **97**:9498-9503.

12 **Coller, H. A., C. Grandori, P. Tamayo, T. Colbert, E. S. Lander, R. N. Eisenman, and T. R. Golub**. 2000. Expression analysis with oligonucleotide microarrays reveals that MYC regulates genes involved in growth, cell cycle, signaling, and adhesion. Proc.Natl.Acad.Sci.U.S.A **97**:3260-3265.

13 **Connell-Crowley, L., J. W. Harper, and D. W. Goodrich**. 1997. Cyclin D1/Cdk4 regulates retinoblastoma protein-mediated cell cycle arrest by site-specific phosphorylation. Mol Biol Cell **8**:287-301.

14 **Cross, S. M., C. A. Sanchez, C. A. Morgan, M. K. Schimke, S. Rame, R. L. Idzerda, W. H. Raskind, and B. J. Reid**. 1995. A p53-dependent mouse spindle checkpoint. Science **267**:1353-1356.

15 **Dang, C. V., L. M. Resar, E. Emison, S. Kim, Q. Li, J. E. Prescott, D. Wonsey, and K. Zeller**. 1999. Function of the c-Myc oncogenic transcription factor. Exp.Cell Res. **253** :63-77.

16 **Deng, C., P. Zhang, J. W. Harper, S. J. Elledge, and P. Leder**. 1995. Mice lacking p21CIP1/WAF1 undergo normal development, but are defective in G1 checkpoint control. Cell **82**:675-684.

17 **Di Leonardo, A., S. P. Linke, K. Clarkin, and G. M. Wahl**. 1994. DNA damage triggers a prolonged p53-dependent G1 arrest and long-term induction of Cip1 in normal human fibroblasts. Genes Dev **8**:2540-51.

18 **Di Leonardo, A., S. P. Linke, Y. Yin, and G. M. Wahl**. 1993. Cell cycle regulation of gene amplification. Cold Spring Harb Symp Quant Biol **58**:655-67.

19 **el-Deiry, W. S., J. W. Harper, P. M. O'Connor, V. E. Velculescu, C. E. Canman, J. Jackman, J. A. Pietenpol, M. Burrell, D. E. Hill, Y. Wang, K. G. Wiman, W. E. Mercer, M. B. Kastan, K. W. E. S. J. Kohn, K. W. Kinzler, and B. Vogelstein**. 1994. WAF1/CIP1 is induced in p53-mediated G1 arrest and apoptosis. Cancer Res **54**:1169-1174.

20 **Facchini, L. M., S. Chen, W. W. Marhin, J. N. Lear, and L. Z. Penn**. 1997. The Myc negative autoregulation mechanism requires Myc-Max association and involves the c-myc P2 minimal promoter. Mol Cell Biol **17**:100-114.

21 **Facchini, L. M. and L. Z. Penn**. 1998. The molecular role of Myc in growth and transformation: recent discoveries lead to new insights. FASEB J **12**:633-651.

22 **Felsher, D. W. and J. M. Bishop**. 1999. Transient excess of MYC activity can elicit genomic instability and tumorigenesis. Proc Natl Acad Sci U S A **96**:3940-3944.

23 **Forrester, H. B., N. Albright, C. C. Ling, and W. C. Dewey**. 2000. Computerized video time-lapse analysis of apoptosis of REC:Myc cells X-irradiated in different phases of the cell cycle. Radiat.Res. **154**:625-639.

24 **Gandarillas, A. and F. M. Watt**. 1997. c-Myc promotes differentiation of human epidermal stem cells. Genes Dev. **11**:2869-2882.

25 **Gudas, J., H. Nguyen, T. Li, D. Hill, and K. H. Cowan**. 1995. Effects of cell cycle, wild-type p53 and DNA damage on p21CIP1/Waf1 expression in human breast epithelial cells. Oncogene **11**:253-261.

26 **Hanson, K. D., M. Shichiri, M. R. Follansbee, and J. M. Sedivy**. 1994. Effects of c-myc expression on cell cycle progression. Mol.Cell Biol. **14**:5748-5755.

27 **Harper, J. W., G. R. Adami, N. Wei, K. Keyomarsi, and S. J. Elledge**. 1993. The p21 Cdk-interacting protein Cip1 is a potent inhibitor of G1 cyclin-dependent kinases. Cell **75**:805-816.

28 **Harrington, E. A., J. L. Bruce, E. Harlow, and N. Dyson**. 1998. pRB plays an essential role in cell cycle arrest induced by DNA damage. Proc Natl Acad Sci U S A **95**:11945-11950.

29 **Hartwell, L.** 1992. Defects in a cell cycle checkpoint may be responsible for the genomic instability of cancer cells. Cell **71**:543-6.

30 **Hermeking, H., C. Lengauer, K. Polyak, T. C. He, L. Zhang, S. Thiagalingam, K. W. Kinzler, and B. Vogelstein**. 1997. 14-3-3 sigma is a p53-regulated inhibitor of G2/M progression. Mol.Cell **1**:3-11.

31 **Jansen-Durr, P., A. Meichle, P. Steiner, M. Pagano, K. Finke, J. Botz, J. Wessbecher, G. Draetta, and M. Eilers**. 1993. Differential modulation of cyclin gene expression by MYC. Proc.Natl.Acad.Sci.U.S.A **90**:3685-3689.

32 **Khan, S. H., J. Moritsugu, and G. M. Wahl**. 2000. Differential requirement for p19ARF in the p53-dependent arrest induced by DNA damage, microtubule disruption, and ribonucleotide depletion. Proc Natl Acad Sci U S A **97**:3266-3271.

33 **Khan, S. H. and G. M. Wahl**. 1998. p53 and pRb prevent rereplication in response to microtubule inhibitors by mediating a reversible G1 arrest. Cancer Res. **58**:396-401.

34 **Kitagawa, M., H. Higashi, H. K. Jung, I. Suzuki-Takahashi, M. Ikeda, K. Tamai, J. Kato, K. Segawa, E. Yoshida, S. Nishimura, and Y. Taya**. 1996. The consensus motif for phosphorylation by cyclin D1-Cdk4 is different from that for phosphorylation by cyclin A/E-Cdk2. EMBO J **15**:7060-7069.

35 **Kiyono, T., S. A. Foster, J. I. Koop, J. K. McDougall, D. A. Galloway, and A. J. Klingelhutz**. 1998. Both Rb/p16INK4a inactivation and telomerase activity are required to immortalize human epithelial cells. Nature **396**:84-88.

36 **Lanni, J. S. and T. Jacks**. 1998. Characterization of the p53-dependent postmitotic checkpoint following spindle disruption. Mol Cell Biol **18**:1055-1064.

37 **Lengauer, C., K. W. Kinzler, and B. Vogelstein**. 1998. Genetic instabilities in human cancers. Nature **396**:643-649.

38 **Li, Q. and C. V. Dang**. 1999. c-Myc overexpression uncouples DNA replication from mitosis. Mol.Cell Biol. **19**:5339-5351.

39 **Littlewood, T. D., D. C. Hancock, P. S. Danielian, M. G. Parker, and G. I. Evan.** 1995. A modified oestrogen receptor ligand-binding domain as an improved switch for the regulation of heterologous proteins. Nucleic Acids Res. **23**:1686-1690.

40 **Livingstone, L. R., A. White, J. Sprouse, E. Livanos, T. Jacks, and T. D. Tlsty.** 1992. Altered cell cycle arrest and gene amplification potential accompany loss of wild-type p53. Cell **70**:923-35.

41 **Liyanage, M., A. Coleman, S. du Manoir, T. Veldman, S. McCormack, R. B. Dickson, C. Barlow, A. Wynshaw-Boris, S. Janz, J. Wienberg, M. A. Ferguson-Smith, E. Schrock, and T. Ried.** 1996. Multicolour spectral karyotyping of mouse chromosomes. Nat Genet **14**:312-5.

42 **Loeb, L. A.** 1991. Mutator phenotype may be required for multistage carcinogenesis. Cancer Res **51**:3075-9.

43 **Mai, S.** 1994. Overexpression of c-myc precedes amplification of the gene encoding dihydrofolate reductase. Gene **148**:253-260.

44 **Mai, S., M. Fluri, D. Siwarski, and K. Huppi.** 1996. Genomic instability in MycER-activated Rat1A-MycER cells. Chromosome Res **4**:365-71.

45 **McCormack, S. J., Z. Weaver, S. Deming, G. Natarajan, J. Torri, M. D. Johnson, M. Liyanage, T. Ried, and R. B. Dickson.** 1998. Myc/p53 interactions in transgenic

mouse mammary development, tumorigenesis and chromosomal instability. Oncogene **16**:2755-2766.

46 **McKenna, W. G., G. Iliakis, M. C. Weiss, E. J. Bernhard, and R. J. Muschel**. 1991. Increased G2 delay in radiation-resistant cells obtained by transformation of primary rat embryo cells with the oncogenes H-ras and v-myc. Radiat.Res. **125**:283-287.

47 **Merlo, G. R., F. Basolo, L. Fiore, L. Duboc, and N. E. Hynes**. 1995. p53-dependent and p53-independent activation of apoptosis in mammary epithelial cells reveals a survival function of EGF and insulin. J Cell Biol **128**:1185-1196.

48 **Meyer, K. M., S. M. Hess, T. D. Tlsty, and S. A. Leadon**. 1999. Human mammary epithelial cells exhibit a differential p53-mediated response following exposure to ionizing radiation or UV light. Oncogene **18**:5795-5805.

49 **Miller, A. D. and G. J. Rosman**. 1989. Improved retroviral vectors for gene transfer and expression. Biotechniques **7**:980-6, 989.

50 **Mitchell, K. O. and W. S. El Deiry**. 1999. Overexpression of c-Myc inhibits p21WAF1/CIP1 expression and induces S-phase entry in 12-O-tetradecanoylphorbol-13-acetate (TPA)-sensitive human cancer cells. Cell Growth Differ. **10**:223-230.

51 **Nass, S. J. and R. B. Dickson**. 1998. Epidermal growth factor-dependent cell cycle progression is altered in mammary epithelial cells that overexpress c-myc. Clin.Cancer Res. **4**:1813-1822.

52 **Paulovich, A. G., D. P. Toczyski, and L. H. Hartwell**. 1997. When checkpoints fail. Cell **88**:315-321.

53 **Penn, L. J., M. W. Brooks, E. M. Laufer, and H. Land**. 1990. Negative autoregulation of c-myc transcription. EMBO J. **9**:1113-1121.

54 **Perez-Roger, I., D. L. Solomon, A. Sewing, and H. Land**. 1997. Myc activation of cyclin E/Cdk2 kinase involves induction of cyclin E gene transcription and inhibition of p27(Kip1) binding to newly formed complexes. Oncogene **14**:2373-2381.

55 **Reisman, D., N. B. Elkind, B. Roy, J. Beamon, and V. Rotter**. 1993. c-Myc trans-activates the p53 promoter through a required downstream CACGTG motif. Cell Growth Differ **4**:57-65.

56 **Shaulian, E., A. Zauberman, D. Ginsberg, and M. Oren**. 1992. Identification of a minimal transforming domain of p53: negative dominance through abrogation of sequence-specific DNA binding. Mol Cell Biol **12**:5581-5592.

57 **Sherr, C. J.** 1998. Tumor surveillance via the ARF-p53 pathway. Genes Dev **12**:2984-2991.

58 **Sherr, C. J. and R. A. DePinho**. 2000. Cellular senescence: mitotic clock or culture shock? Cell **102**:407-410.

59 **Soule, H. D., T. M. Maloney, S. R. Wolman, W. D. J. Peterson, R. Brenz, C. M. McGrath, J. Russo, R. J. Pauley, R. F. Jones, and S. C. Brooks**. 1990. Isolation and characterization of a spontaneously immortalized human breast epithelial cell line, MCF-10. Cancer Res **50**:6075-6086.

60 **Spotts, G. D., S. V. Patel, Q. Xiao, and S. R. Hann**. 1997. Identification of downstream-initiated c-Myc proteins which are dominant-negative inhibitors of transactivation by full-length c-Myc proteins. Mol.Cell Biol. **17**:1459-1468.

61 **Stampfer, M. R. and J. C. Bartley**. 1985. Induction of transformation and continuous cell lines from normal human mammary epithelial cells after exposure to benzo[a]pyrene. Proc Natl Acad Sci U S A **82**:2394-2398.

62 **Stampfer, M. R., C. H. Pan, J. Hosoda, J. Bartholomew, J. Mendelsohn, and P. Yaswen**. 1993. Blockage of EGF receptor signal transduction causes reversible arrest of normal and immortal human mammary epithelial cells with synchronous reentry into the cell cycle. Exp Cell Res **208**:175-188.

63 **Stewart, Z. A., S. D. Leach, and J. A. Pietenpol**. 1999. p21(Waf1/Cip1) inhibition of cyclin E/Cdk2 activity prevents endoreduplication after mitotic spindle disruption. Mol.Cell Biol. **19**:205-215.

64 **Tait, L., H. D. Soule, and J. Russo** . 1990. Ultrastructural and immunocytochemical characterization of an immortalized human breast epithelial cell line, MCF-10. Cancer Res **50**:6087-6094.

65 **Valverius, E. M., F. Ciardiello, N. E. Heldin, B. Blondel, G. Merlo, G. Smith, M. R. Stampfer, M. E. Lippman, R. B. Dickson, and D. S. Salomon**. 1990. Stromal influences on transformation of human mammary epithelial cells overexpressing c-myc and SV40T. J.Cell Physiol **145**:207-216.

66 **Vidair, C. A., C. H. Chen, C. C. Ling, and W. C. Dewey**. 1996. Apoptosis induced by X-irradiation of rec-myc cells is postmitotic and not predicted by the time after irradiation or behavior of sister cells. Cancer Res. **56**:4116-4118.

67 **Wahl, G. M., S. P. Linke, T. G. Paulson, and L. C. Huang**. 1997. Maintaining genetic stability through TP53 mediated checkpoint control. Cancer Surv **29**:183-219.

68 **Waldman, T., K. W. Kinzler, and B. Vogelstein**. 1995. p21 is necessary for the p53-mediated G1 arrest in human cancer cells. Cancer Res **55**:5187-5190.

69 **Waldman, T., C. Lengauer, K. W. Kinzler, and B. Vogelstein**. 1996. Uncoupling of S phase and mitosis induced by anticancer agents in cells lacking p21. Nature **381**:713-716.

70 **Weaver, Z. A., S. J. McCormack, M. Liyanage, M. S. du, A. Coleman, E. Schrock, R. B. Dickson, and T. Ried**. 1999. A recurring pattern of chromosomal aberrations in mammary gland tumors of MMTV-cmyc transgenic mice. Genes Chromosomes Cancer **25**:251-260.

71 **Xiong, Y., G. J. Hannon, H. Zhang, D. Casso, R. Kobayashi, and D. Beach**. 1993. p21 is a universal inhibitor of cyclin kinases. Nature **366**:701-704.

72 **Yin, Y., M. A. Tainsky, F. Z. Bischoff, L. C. Strong, and G. M. Wahl**. 1992. Wild-type p53 restores cell cycle control and inhibits gene amplification in cells with mutant p53 alleles. Cell **70**:937-48.

73 **Zindy, F., C. M. Eischen, D. H. Randle, T. Kamijo, J. L. Cleveland, C. J. Sherr, and M. F. Roussel**. 1998. Myc signaling via the ARF tumor suppressor regulates p53-dependent apoptosis and immortalization. Genes Dev **12**:2424-2433.

Figure Legends

Figure 1. Abrogation of G1/S arrest following γ-irradiation in c-Myc-overexpressing 184A1N4 HMECs.

Flow cytometric profiles representing cell cycle changes of A1N4 (parental HMECs) or A1N4-Myc (c-Myc-overexpressing HMECs) after 24hr post-IR incubation. DNA-content flow cytometric analysis, measuring the amount of fluorescent dye (propidium iodide) intercalated into DNA, provides a readout for the distribution of cells with different DNA contents in the population. DNA content is represented on the x axis, and the number of cells counted is represented on the y axis. The relative amounts of different peaks on the readout indicates the fraction of the cell population in different phases of the cell cycle; G0/G1 (2N content), S (intermediate between 2N and 4N), and G2/M (4N content). Before IR treatment, A1N4 and A1N4-Myc cells were synchronized in G0/G1 phase through an EGF withdrawal method. After a post-release recovery for 3 hrs in complete media containing EGF, HMECs were irradiated with 0, 6, 12, and 24 Gray doses of IR to induce DNA damage. HMECs were then allowed to progress in the cell cycle during 24hr post-IR incubation.

Figure 2. Retroviral constructs

(A) Protein structure of human c-Myc. c-Myc has well separated functional domains in its amino (N)-terminus and its carboxy (C)-terminus. The C-terminal structure promotes the essential DNA binding activity through the heterodimer formation with Max. Basic (B), Helix-Loop-Helix (HLH), and Leucine Zipper (LZ) regions, represented as

shadowed boxes in the C-terminus, are essential to Myc-Max heterodimerization. The N-terminal structure determines the transcription regulatory activity of c-Myc. This transcription regulatory domain (TRD), represented as shadowed region in N-terminus, contains a highly conserved Myc-Box I (MB-I, amino acids 45 to 63) and Myc-Box II (MB-II, amino acids 129 to 141) sequences. Myc1 (67kDa) and Myc2 (64kDa) initiate their translation at the first start codon (CUG) and at the second start codon (AUG) located upstream of MB-I sequence. However, when translation is initiated at the third start codon (the second AUG), it produces a truncated form of c-Myc (c-MycS, 46kDa) without a MB-I sequence since the internal start codon is located downstream of MB-I. (B) Schematic maps of retroviral constructs used in this study. pLXSN (LTR-Gene X-SV40-Neo) retroviral vector has two promoters (5′ MoMuSV-LTR directs transcription of gene X at MCS, containing *Eco*RI and *Hpa*I sites, and SV40 early promoter (SV) directs transcription of neomycin resistance gene (NEO)). The dotted lines in pLXSN-MycS and pLXSN-p53DD represent the deleted sequences in each construct. c-MycS was created, based on the full-length c-Myc construct (see Materials and Methods for details). Polyadenylation of the exogenous mRNA transcript is mediated by the polyadenylation signal (pA) in 3′ MoMuLV-LTR. (C) Immunoblot analysis for exogenous human c-Myc and c-MycS proteins in c-Myc- or c-MycS-infected MCF10A and NIH3T3 cells. Anti-human c-Myc monoclonal antibody 9E10 detected endogenous human c-Myc in MCF10A-LXSN and failed to detect murine c-Myc in NIH3T3 cells. Production of c-MycS appeared to be tightly regulated; it is only apparent in cells with deregulated c-Myc and c-MycS. Equal loading was confirmed by staining the membrane blot with

amido-black (data not shown). (D) Immunoblot analysis for p53 proteins in the retrovirus-infected MCF10A HMECs. Overexpression of murine p53DD (~19 kDa) in p53DD-infected MCF10A cells was clearly detected with an anti-Pan-species p53 C-terminal monoclonal antibody, PAb421. The accompanying increase of endogenous full-length human p53 (53 kDa) suggests the efficient binding of p53DD to endogenous p53. The same blot was reprobed with anti-p21/WAF1 antibody and served to confirm the absence of p53 function in p53DD-infected cells. Equal loading was confirmed by staining the membrane blot with amido-black (data not shown). (E) Proliferation of the infected MCF10A HMECs was measured using a 96-well plate assay. The x axis represents incubation time after plating on the 96-well culture plate and the y axis represents an arbitrary unit of optical density at 570 nm wavelength. After crystal violet staining of cells on the plates at each time point, stained total cell proteins were dissolved in the sodium citrate solutions and the absorption at 570 nm was measured as a readout for cell proliferation. Error bars indicate the standard deviations calculated from the sextuplicate samples.

Figure 3. c-Myc attenuates G1/S arrest following γ-irradiation in MCF10A HMECs.

(A) Flow cytometric profiles representing cell cycle changes of MCF10A-LXSN, MCF10A-Myc, MCF10A-MycS, or MCF10A-p53DD cells, following IR. The x axis represents DNA content and the y axis represents the number of cells counted. Asynchronous, exponentially growing, cell populations were harvested and irradiated in suspension with 0 or 12 Gray IR. Next, infected cells were allowed to progress in the

cell cycle for 24 hrs or 48 hrs of post-IR incubation. Primary histogram data are displayed as fine line graphs, and the computer-generated, best fit is shown with the orange ~~shadowed~~ (G0/G1 and G2/M) and the dashed (S phase) areas. (B) BrdU incorporation assay for *de novo* DNA synthesis using anti-BrdU immunofluorescence of non-irradiated cells or 12 Gray IR-irradiated cells. Treatment with IR was essentially the same as in the flow cytometric analyses. Following γ-irradiation of suspended cells, cells were replated and allowed a 24hr post-IR incubation before the additional 24hr incubation with BrdU. After immunofluorescence staining with fluorescein-linked anti-BrdU monoclonal antibody (αBrdU) for nuclei undergone *de novo* DNA synthesis, all nuclei were counterstained with non-specific DNA intercalating dye, propidium iodide (PI), to allow quantification of the total number of nuclei in the same microscopic field. At least 300 PI-stained nuclei were analyzed for each infected population with image analysis software.

Figure 4. Time-course analysis of changes in cell cycle-related proteins following γ-irradiation.

(A) Immunoblot analysis for c-Myc, Rb, or Cyclin A in whole cell lysates prepared at indicated time points after 12 Gray IR. All cells were irradiated, and 0 hr post-IR time-point lysates were prepared immediately following γ-irradiation. An equal loading control is provided by the α-tubulin blot. The same membrane was reprobed repeatedly to acquire immunoblot results for each protein. Hyperphosphorylated Rb (ppRB) in the

slow migrating bands and hypophosphorylated Rb (pRB) in the fast migrating bands are indicated. (B) Immunoblot analyses for p53 and p21/Cip1 in whole cell lysates prepared at indicated time points after 12 Gray IR. An equal loading control is provided by the Max blot. The same membrane was reprobed repeatedly to acquire immunoblot results for each protein.

Figure 5. Regulatable c-Myc system in MCF10A HMECs.

(A) Immunoblot analysis confirms protein expression of MycER™ in MCF10A HMEC. After 48 hrs of EtOH or 1 μM 4-OHT treatment, total cell lysates were prepared and separated in SDS-PAGE. (B) Phase contrast microscopy of MCF10A-LXSN and MCF10A-MycER™, after 6 days of EGF starvation, in the presence of EtOH or 1μM 4-OHT. EtOH-treated MCF10A-MycER™ cells showed severely flattened cellular morphology in the absence of EGF. 4-OHT-treated MCF10A-MycER™ cells demonstrated a marked increase of floating bodies and slender cellular morphology (yellow arrows). (C) A Hoechst 33258 staining assay demonstrated EGF starvation-induced apoptosis only in cells with excess c-Myc activity. MCF10A-LXSN and MCF10A-MycER™ were EGF-starved for 6 days in the presence of EtOH or 1μM 4-OHT. Mitotic chromosomes (white arrow) were clearly distinguished from apoptotic nuclei (yellow arrows). (D) Fragmented and condensed nuclei (yellow arrow) resulting from c-Myc-induced apoptosis in the EGF-starved HMECs.

Figure 6. Transient excess of c-Myc activity attenuates the IR-induced G1/S arrest in

MCF10A HMECs.

BrdU incorporation assay for *de novo* DNA synthesis of MCF10A-MycER™ cells following IR. Treatment of IR was essentially the same as that in the stably-transfected MCF10A HMECs. Following the harvest of asynchronous exponentially growing cells, cells were irradiated in suspension and replated for 24hr post-IR incubation in the presence of EtOH or 1μM 4-OHT, before an additional 24hr incubation with BrdU under the same treatment conditions. After immunofluorescence staining with fluorescein-linked anti-BrdU monoclonal antibody (αBrdU) to detect nuclei that had undergone *de novo* DNA synthesis, all nuclei were counterstained with non-specific DNA intercalating dye, 4', 6'-diamidino-2-phenylindole (DAPI), to quantify the total number of nuclei in the same microscopic field. At least 150 DAPI-stained nuclei were analyzed for each treated population with image analysis software.

Figure 7. Overexpression of c-Myc attenuates the IR-induced G1/S arrest in normal HMECs with a finite lifespan.

(A) Transient infection of normal HMECs with recombinant retroviruses. After 48hr post infection, total cell lysates were prepared and probed with each specific antibody. An equal loading control is provided by the α-tubulin blot. (B) Phase contrast microscopy showing morphological changes of non-infected (None) or transiently infected normal HMECs after 0 Gray or 12 Gray IR. (C) BrdU incorporation assay for *de novo* DNA synthesis of normal HMECs after IR. Retroviral infection and IR were applied directly to the attached cells on the glass cover slip (see Material and Methods).

At least 300 DAPI-stained nuclei were analyzed for each population with image analysis software. Error bars represent the standard deviation calculated from three samples. (D) Representative figures for BrdU incorporation following 0 Gray or 12 Gray IR in normal HMECs. After BrdU staining, all nuclei were counterstained with 4', 6'-diamidino-2-phenylindole (DAPI), to count the total number of nuclei in the same microscopic field.

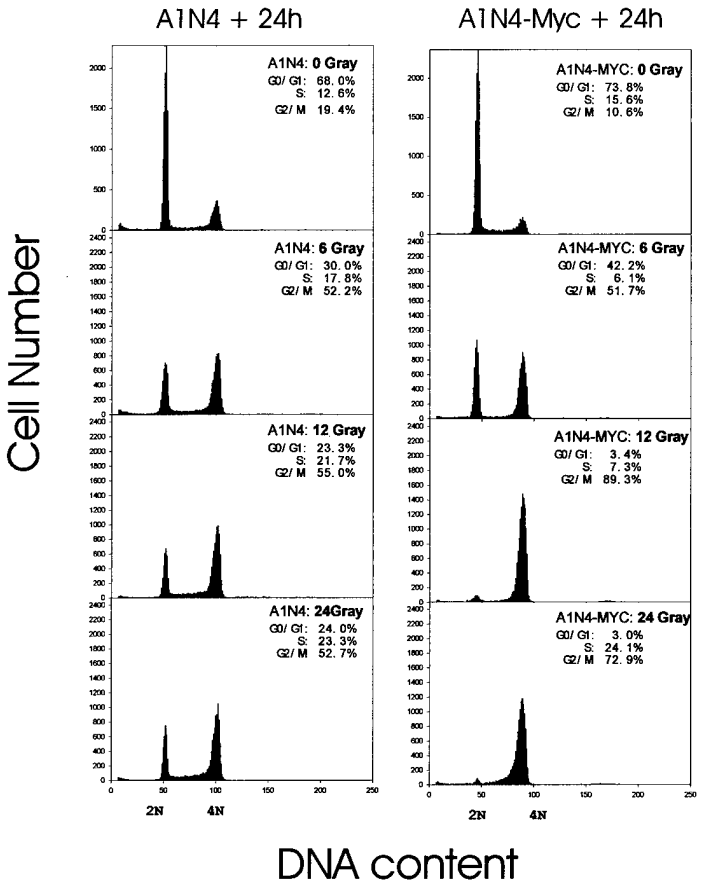
A1N4 + 24h
A1N4-Myc + 24h
A1N4: 0 Gray
G0/ G1: 68. 0%
S: 12. 6%
G2/ M 19. 4%
A1N4: 6 Gray
G0/ G1: 30. 0%
S: 17. 8%
G2/ M 52. 2%
A1N4: 12 Gray
G0/ G1: 23. 3%
S: 21. 7%
G2/ M 55. 0%
A1N4: 24Gray
G0/ G1: 24. 0%
S: 23. 3%
G2/ M 52. 7%
A1N4-MYC: 0 Gray
G0/ G1: 73. 8%
S: 15. 6%
G2/ M 10. 6%
A1N4-MYC: 6 Gray
G0/ G1: 42. 2%
S: 6. 1%
G2/ M 51. 7%
A1N4-MYC: 12 Gray
G0/ G1: 3. 4%
S: 7. 3%
G2/ M 89. 3%
A1N4-MYC: 24 Gray
G0/ G1: 3. 0%
S: 24. 1%
G2/ M 72. 9%
2N
4N
Cell Number
DNA content

Fig 1

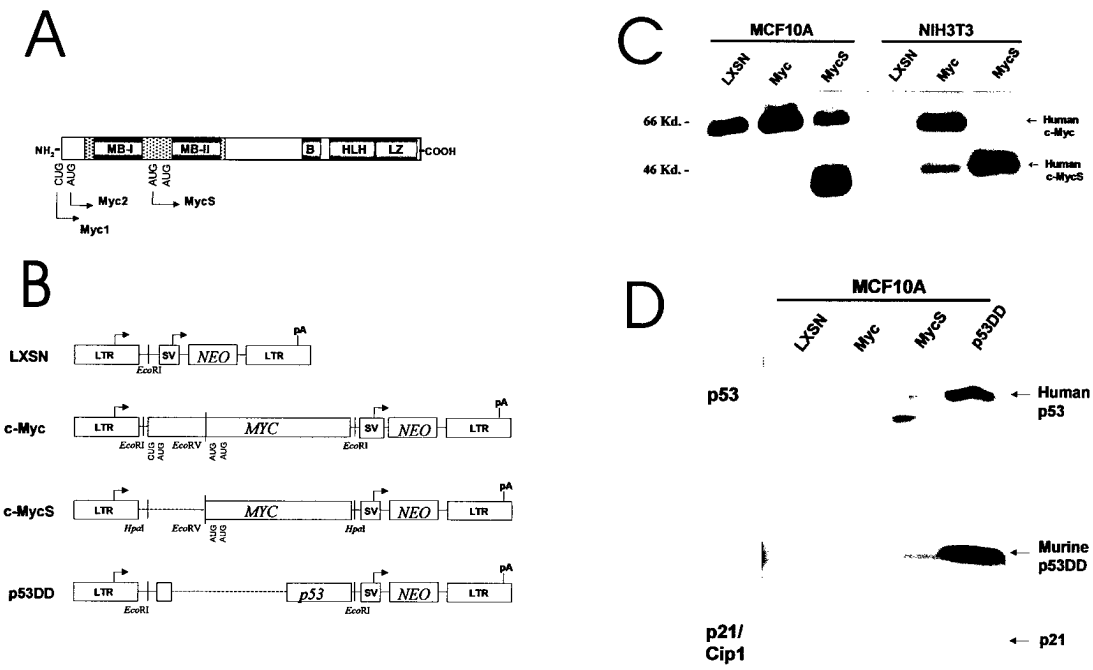
A
NH2-
MB-I
MB-II
B
HLH
LZ
-COOH
CUG
AUG
AUG
AUG
Myc2
MycS
Myc1
B
LXSN
LTR
SV
NEO
LTR
pA
EcoRI
c-Myc
MYC
EcoRV
c-MycS
HpaI
p53DD
p53
C
MCF10A
NIH3T3
LXSN
Myc
MycS
66 Kd. -
46 Kd. -
Human c-Myc
Human c-MycS
D
MCF10A
LXSN
Myc
MycS
p53DD
p53
Human p53
Murine p53DD
p21/ Cip1
p21

E

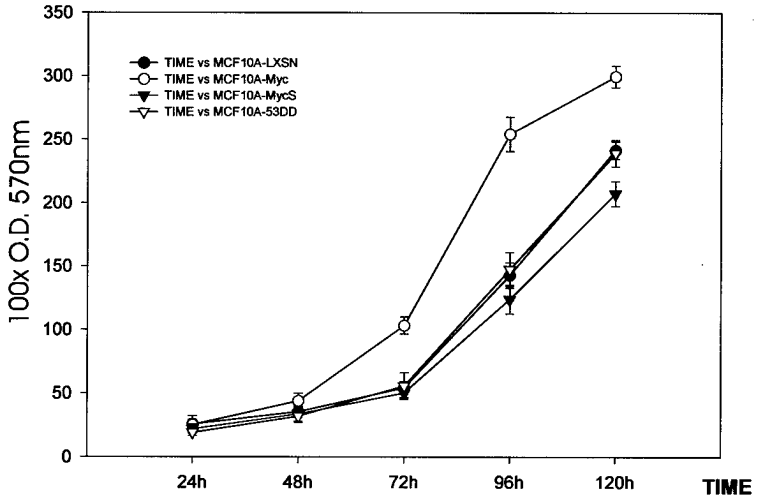
TIME vs MCF10A-LXSN
TIME vs MCF10A-Myc
TIME vs MCF10A-MycS
TIME vs MCF10A-53DD
100x O.D. 570nm
350
300
250
200
150
100
50
0
24h
48h
72h
96h
120h
TIME

Fig 2

A

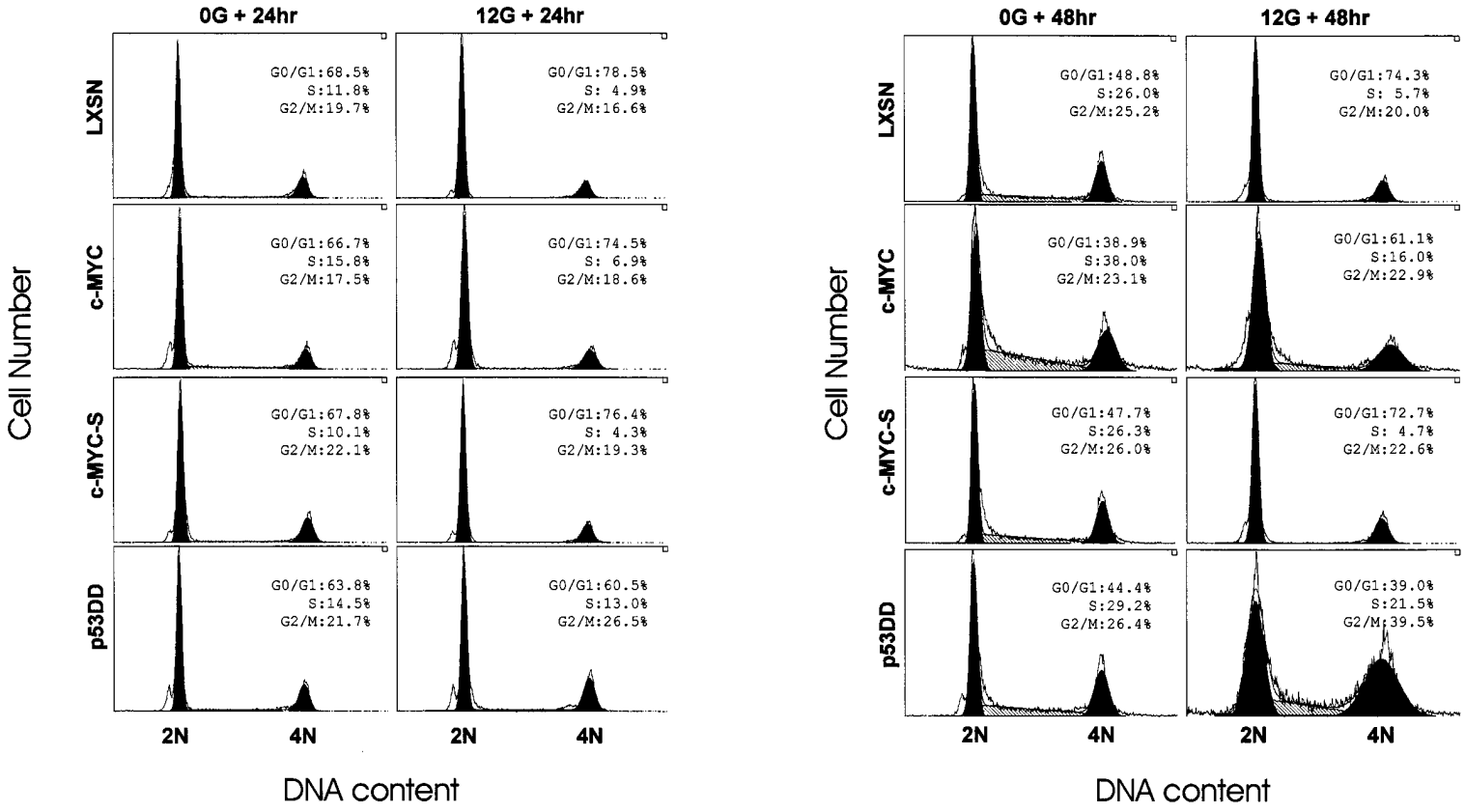
0G + 24hr
12G + 24hr
0G + 48hr
12G + 48hr
LXSN
c-MYC
c-MYC-S
p53DD
G0/G1:68.5%
S:11.8%
G2/M:19.7%
G0/G1:78.5%
S: 4.9%
G2/M:16.6%
G0/G1:48.8%
S:26.0%
G2/M:25.2%
G0/G1:74.3%
S: 5.7%
G2/M:20.0%
G0/G1:66.7%
S:15.8%
G2/M:17.5%
G0/G1:74.5%
S: 6.9%
G2/M:18.6%
G0/G1:38.9%
S:38.0%
G2/M:23.1%
G0/G1:61.1%
S:16.0%
G2/M:22.9%
G0/G1:67.8%
S:10.1%
G2/M:22.1%
G0/G1:76.4%
S: 4.3%
G2/M:19.3%
G0/G1:47.7%
S:26.3%
G2/M:26.0%
G0/G1:72.7%
S: 4.7%
G2/M:22.6%
G0/G1:63.8%
S:14.5%
G2/M:21.7%
G0/G1:60.5%
S:13.0%
G2/M:26.5%
G0/G1:44.4%
S:29.2%
G2/M:26.4%
G0/G1:39.0%
S:21.5%
G2/M:39.5%
2N
4N
Cell Number
DNA content

B

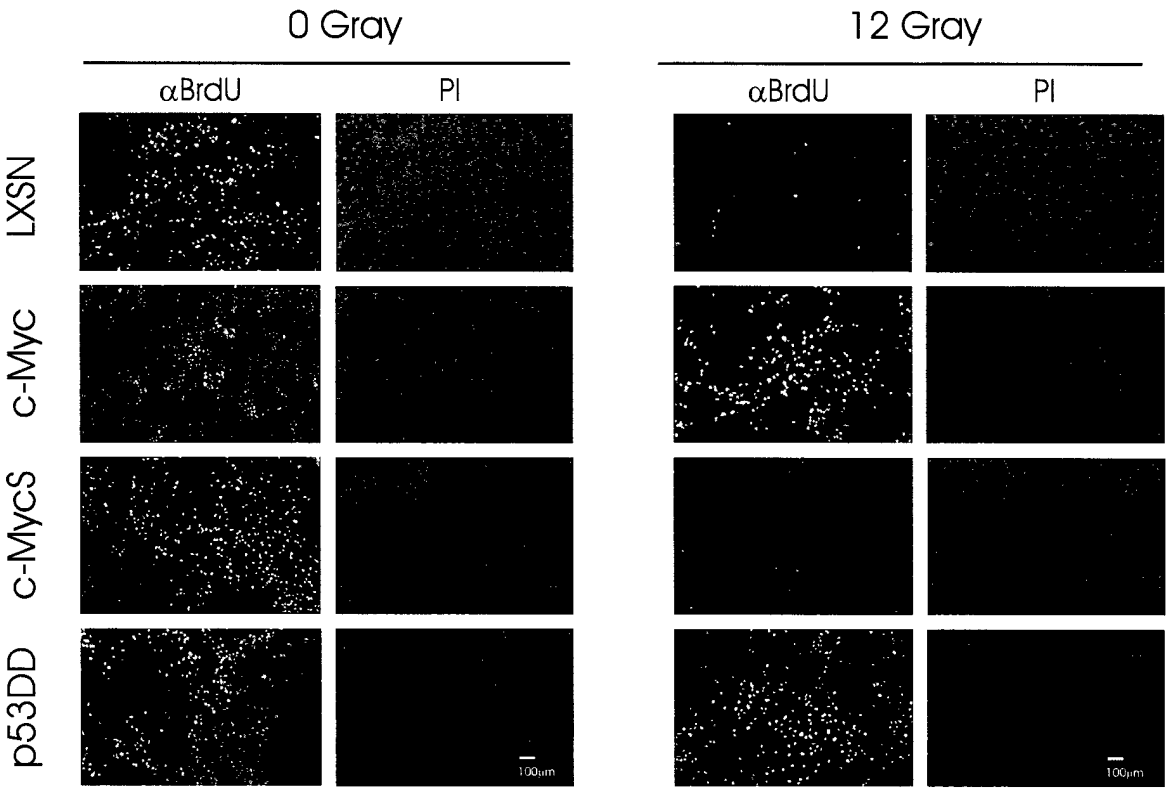
0 Gray
12 Gray
αBrdU
PI
αBrdU
PI
LXSN
c-Myc
c-MycS
p53DD
100μm
100μm

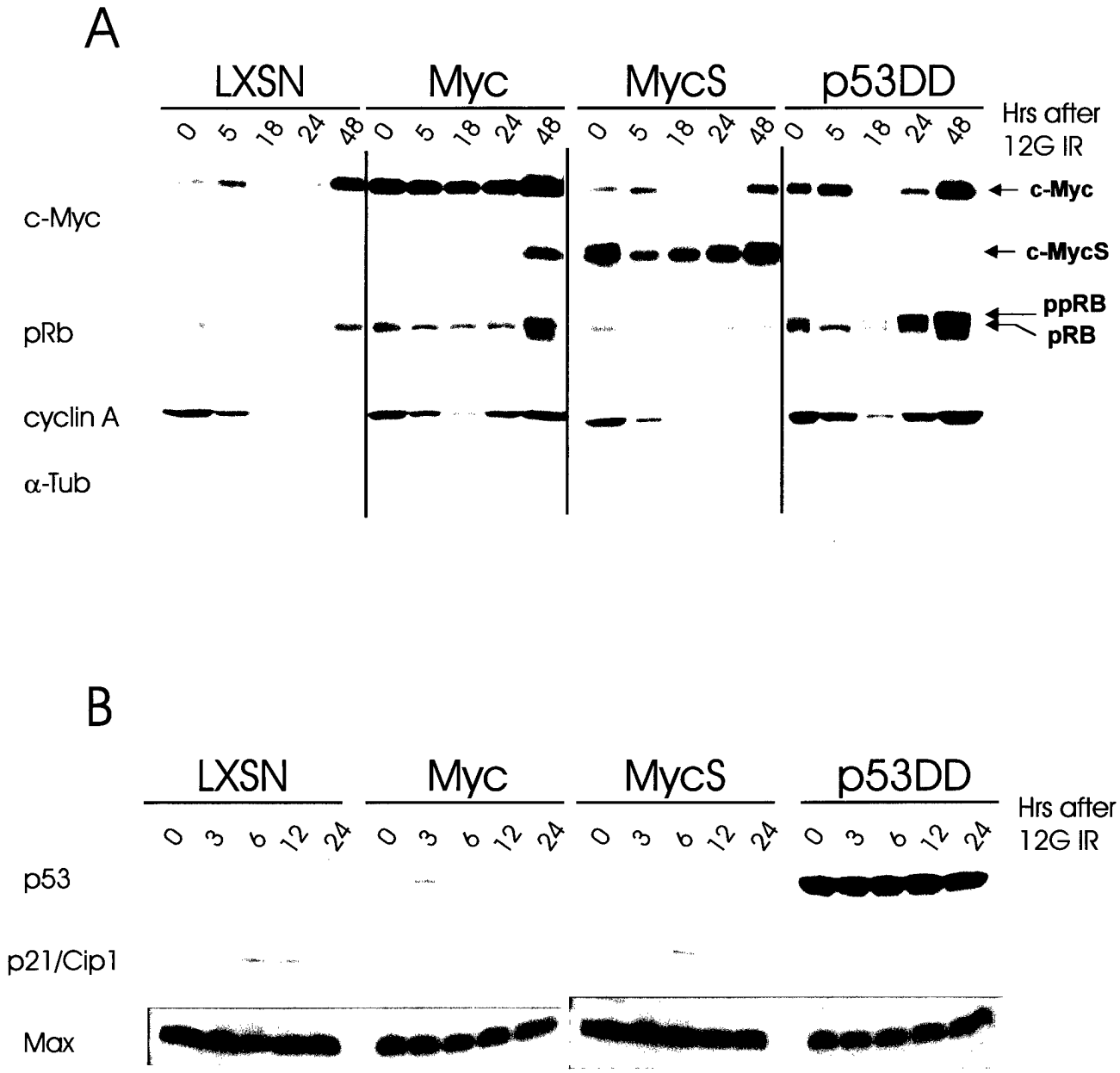
A
LXSN
Myc
MycS
p53DD
0 5 18 24 48
Hrs after 12G IR
c-Myc
pRb
cyclin A
α-Tub
c-Myc
c-MycS
ppRB
pRB
B
LXSN
Myc
MycS
p53DD
0 3 6 12 24
Hrs after 12G IR
p53
p21/Cip1
Max

Fig 4

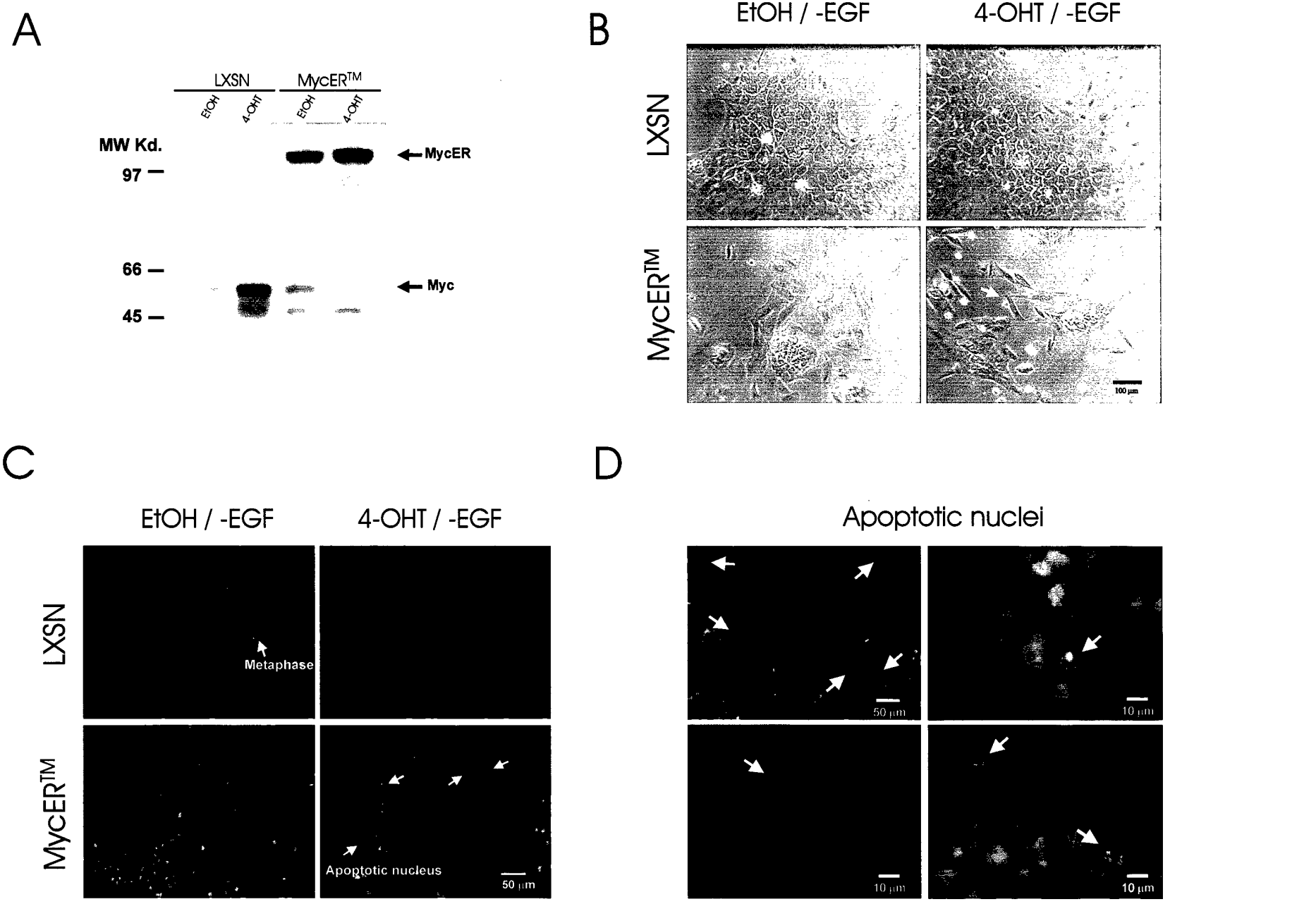
A
LXSN
MycER™
EtOH
4-OHT
EtOH
4-OHT
MW Kd.
97
66
45
MycER
Myc
B
EtOH / -EGF
4-OHT / -EGF
LXSN
MycER™
100 µm
C
EtOH / -EGF
4-OHT / -EGF
LXSN
MycER™
Metaphase
Apoptotic nucleus
50 µm
D
Apoptotic nuclei
50 µm
10 µm
10 µm
10 µm

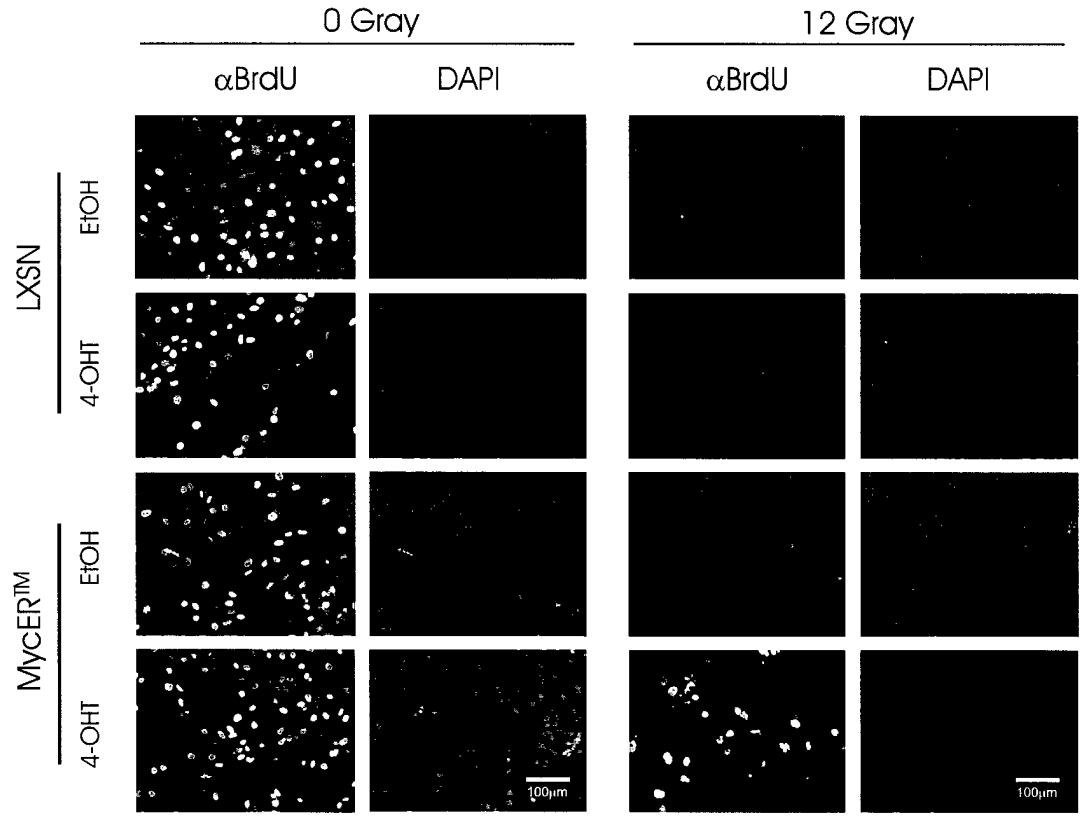
0 Gray
12 Gray
αBrdU
DAPI
αBrdU
DAPI
LXSN
EtOH
4-OHT
MycER™
EtOH
4-OHT
100µm
100µm

A

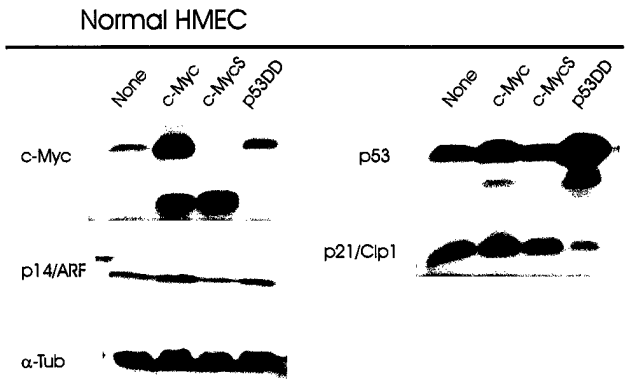
Normal HMEC
None
c-Myc
c-MycS
p53DD
c-Myc
p14/ARF
α-Tub
None
c-Myc
c-MycS
p53DD
p53
p21/Clp1

B

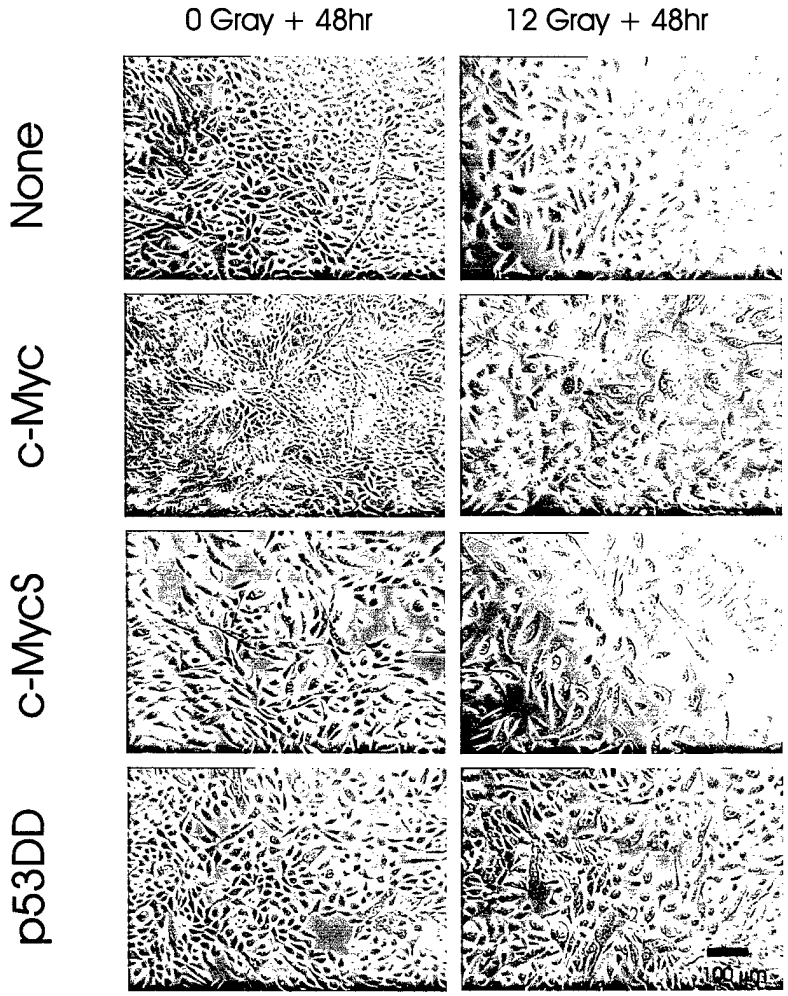
0 Gray + 48hr
12 Gray + 48hr
None
c-Myc
c-MycS
p53DD

C

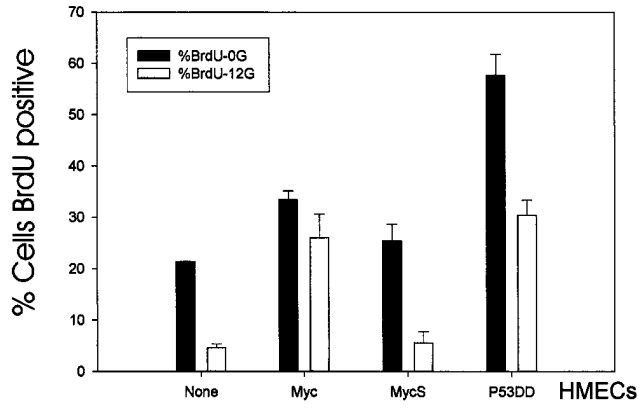
% Cells BrdU positive
70
60
50
40
30
20
10
0
%BrdU-0G
%BrdU-12G
None
Myc
MycS
P53DD
HMECs

D

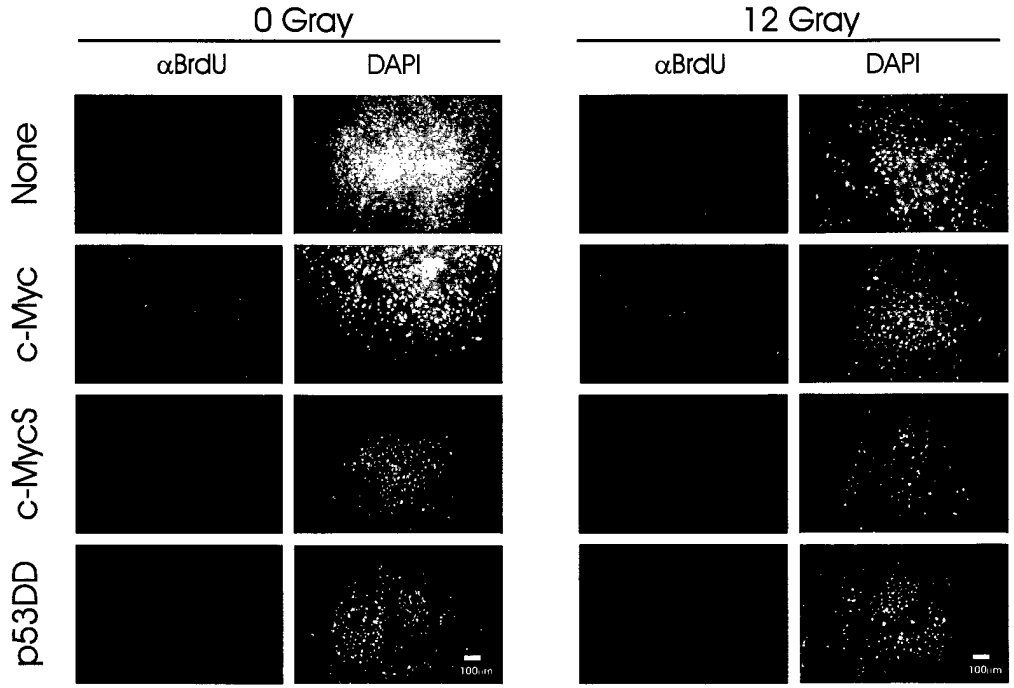
0 Gray
12 Gray
αBrdU
DAPI
αBrdU
DAPI
None
c-Myc
c-MycS
p53DD
100μm
100μm